

Searching for New Physics through Higgs Boson Pair Production

Allison McCarn Deiana

Southern Methodist University

1

Introduction to the Standard Model

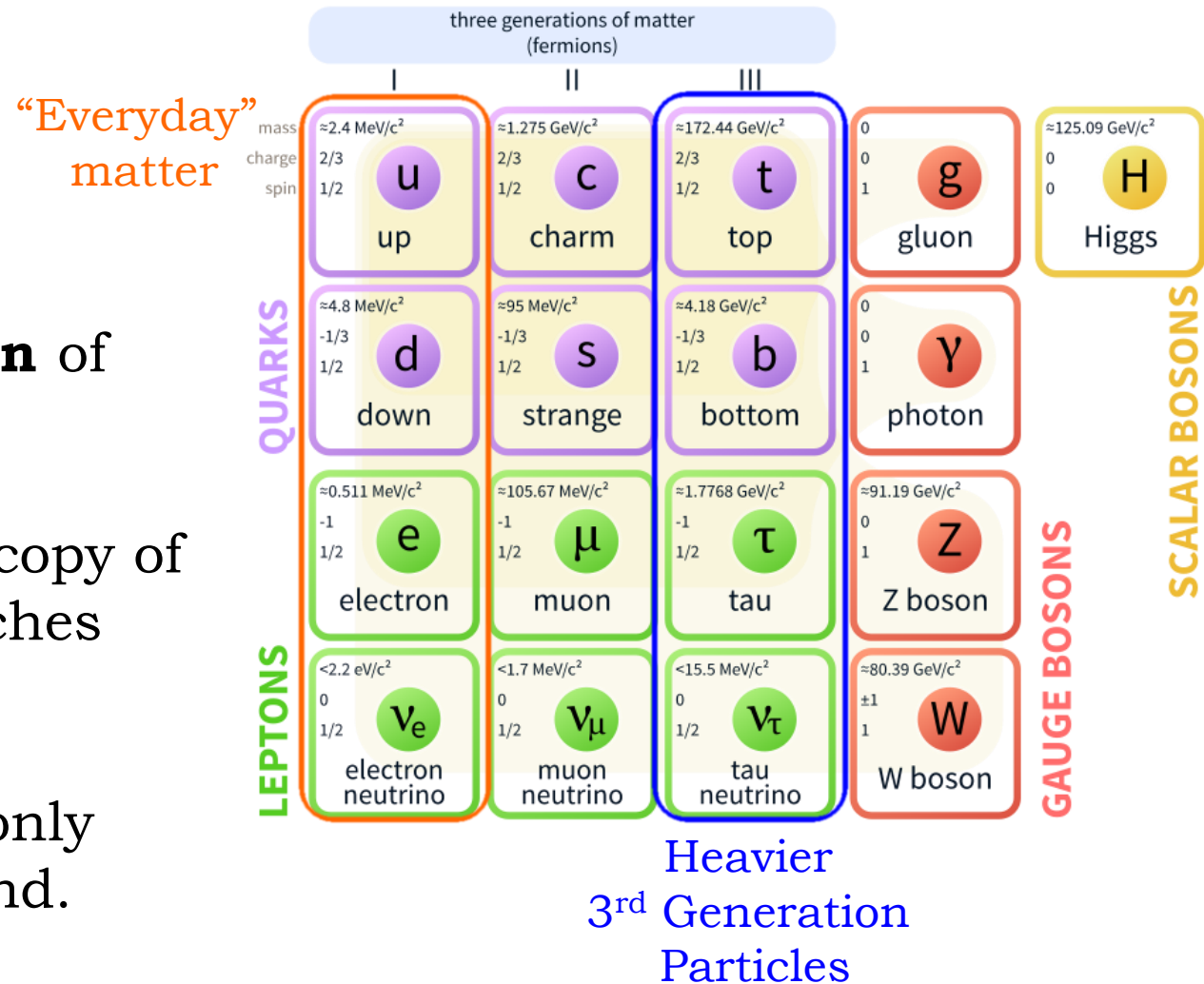
The **Standard Model** has been successful in predicting observational results.

Matter we see around us is only composed from the **first generation** of particles.

The **third generation** is a heavier copy of the first → important in many searches for new particles with colliders.

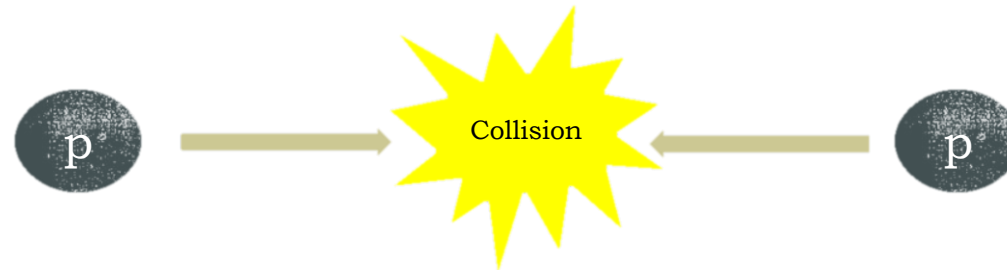
Before the Large Hadron Collider, only the **Higgs boson** had not been found.

Standard Model of Elementary Particles



The Large Hadron Collider (LHC)

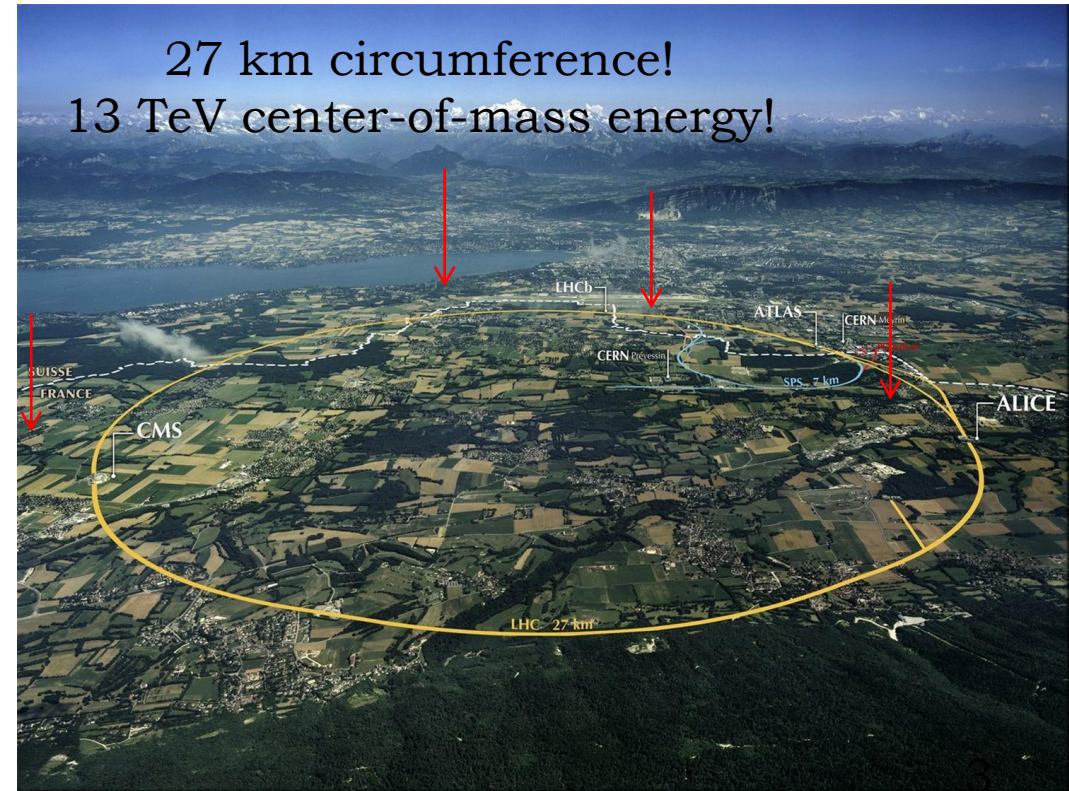
In high energy particle physics, we use **huge machines** operating with **high energy densities** to investigate the smallest pieces of our universe.



The LHC accelerates protons to speed of light, and smashes them together.

The energy of these collisions can produce **heavy particles**, which decay into lighter particles.

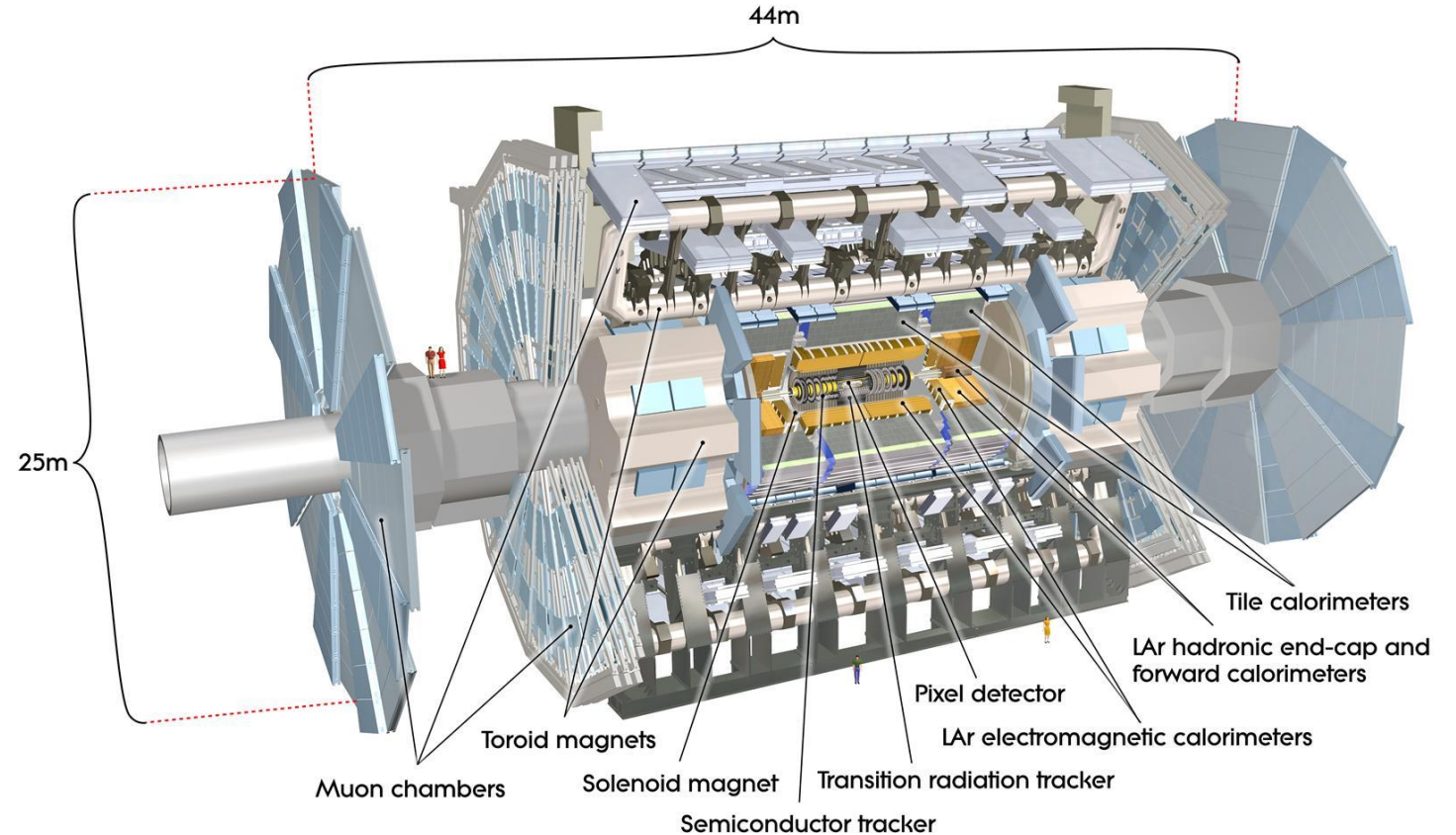
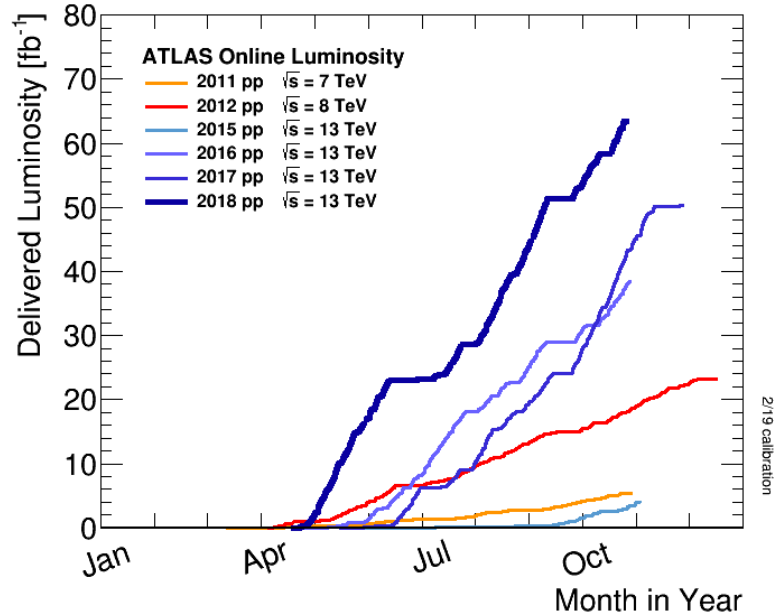
This way, we can investigate the behavior of particles we don't see every day!



The ATLAS Detector

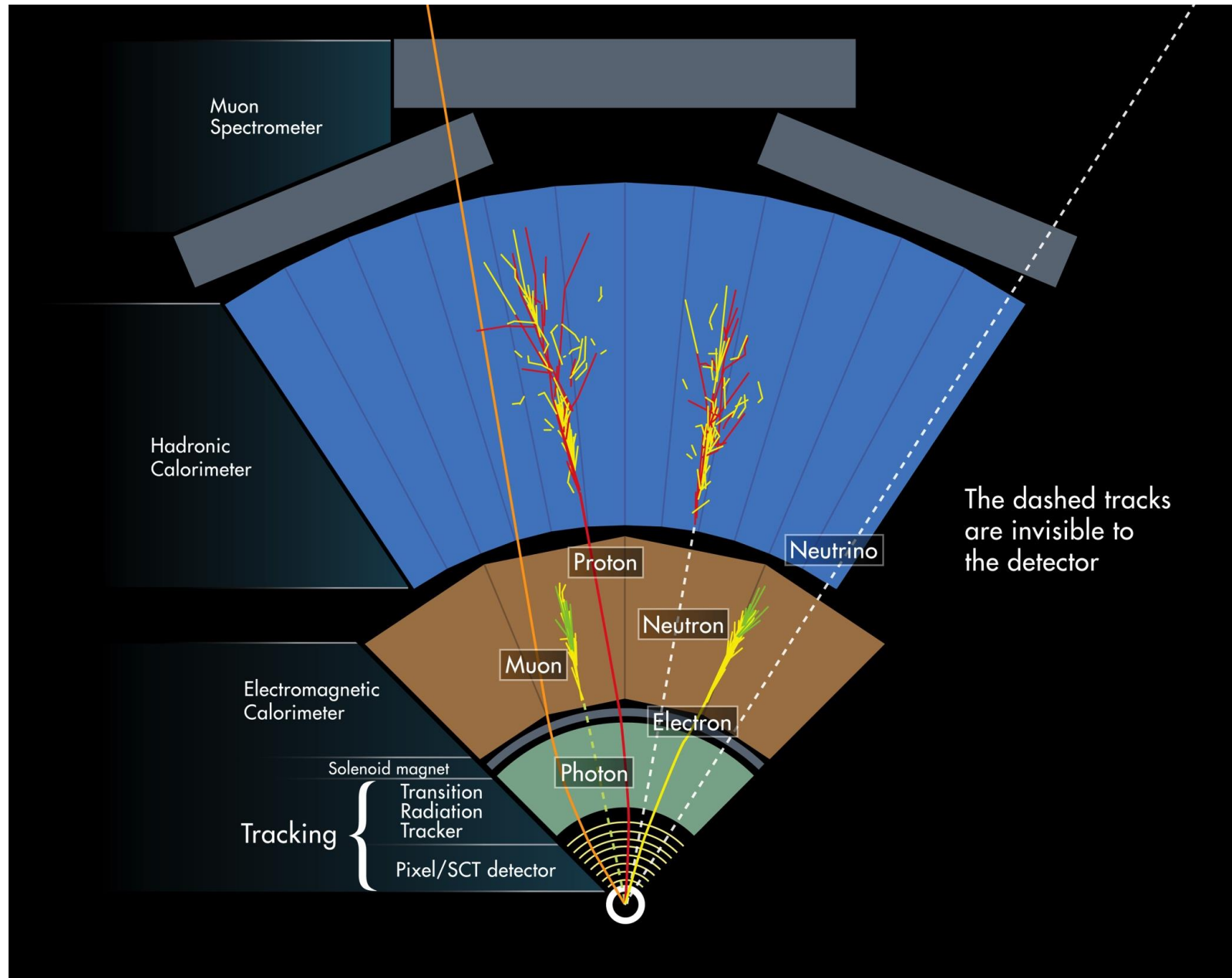
Want to visit ATLAS? You can explore the detector via virtual reality!

<https://atlasrift.web.cern.ch/>



The research presented today is conducted with pp collision data produced at $\sqrt{s} = 13$ TeV by the LHC and recorded by the ATLAS Detector.

The ATLAS Detector, Cross Section

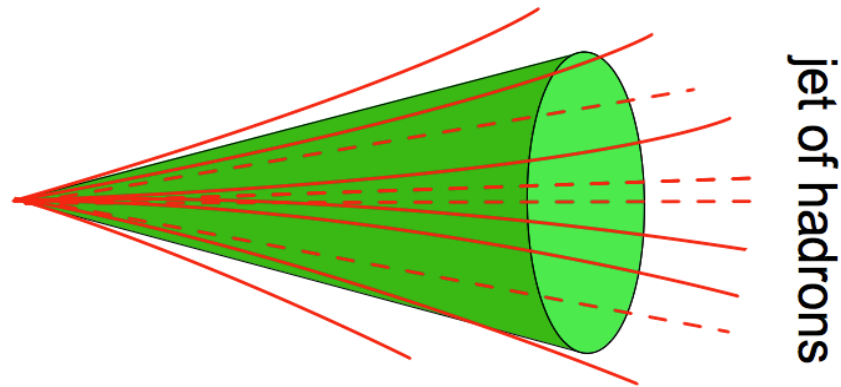


Terminology: Jets in the ATLAS Detector

Proton-proton collisions at the LHC frequently produce **quarks** and **gluons**.

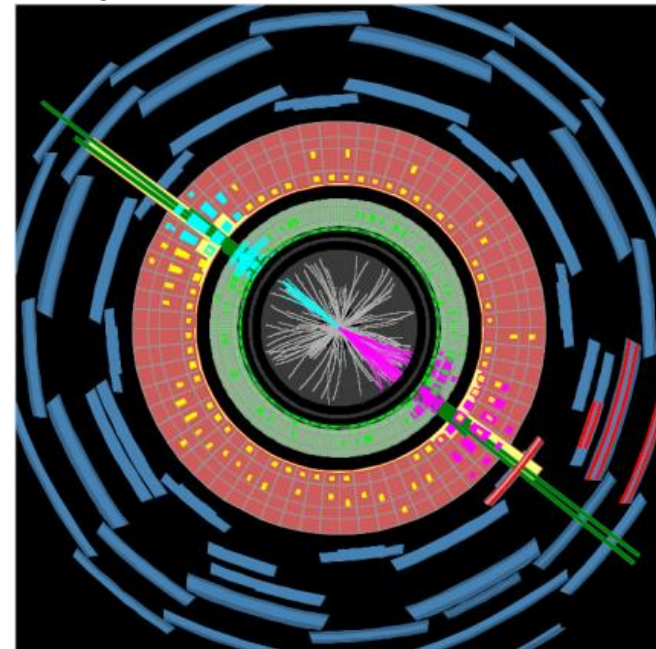
These particles cannot remain free (due to the strong force), so they quickly combine with one another to form non-elementary SM particles (**'hadrons'**).

This process generates a stream of particles that is detected by the ATLAS detectors trackers and calorimeters, and which is called a **"jet"**.



Visualization of a jet

Actual jets in the ATLAS Detector

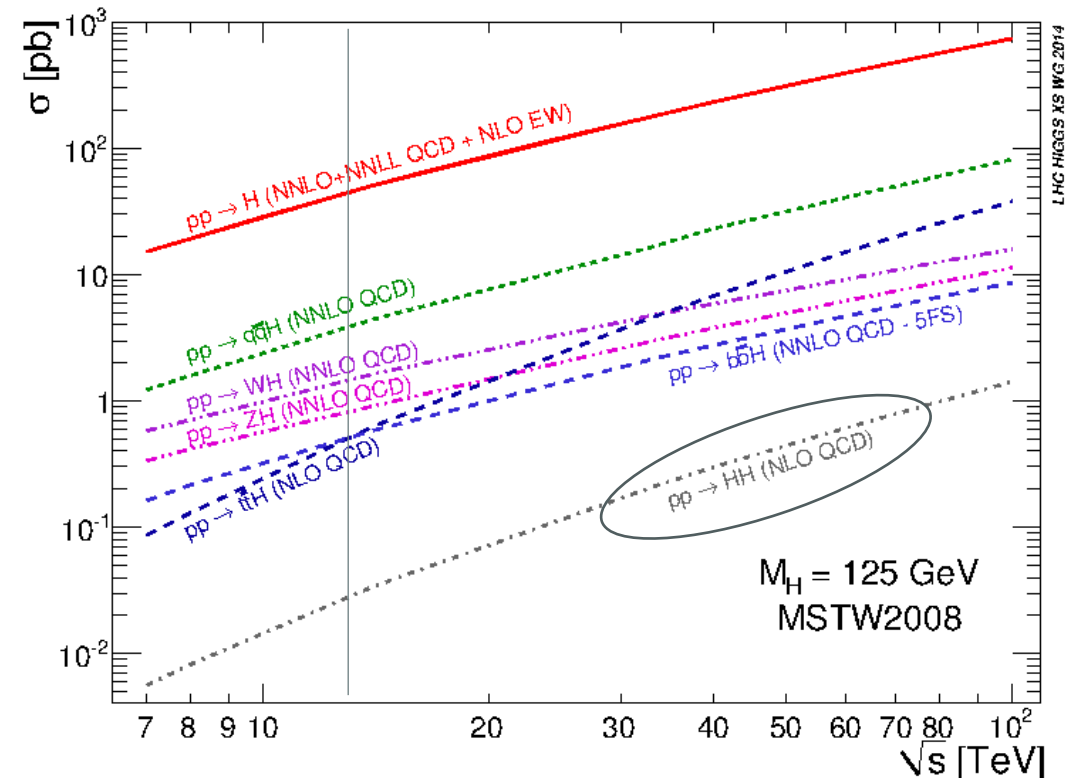
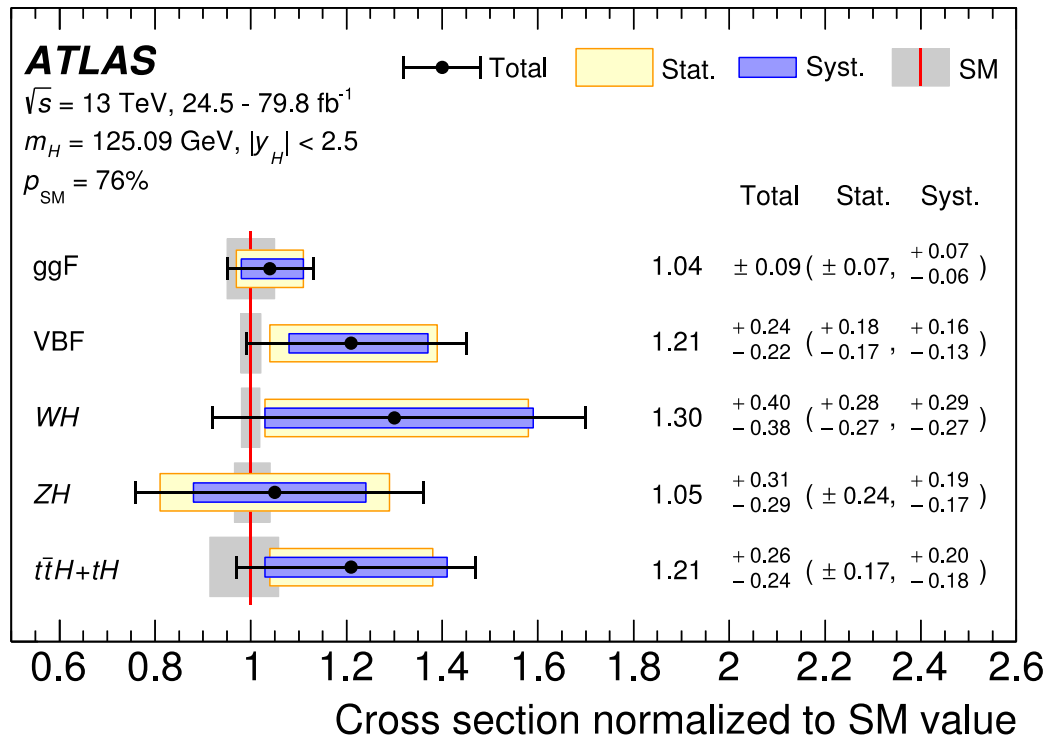


The Higgs Boson at the LHC

The observation of an SM-like Higgs boson is a major success of the LHC program.

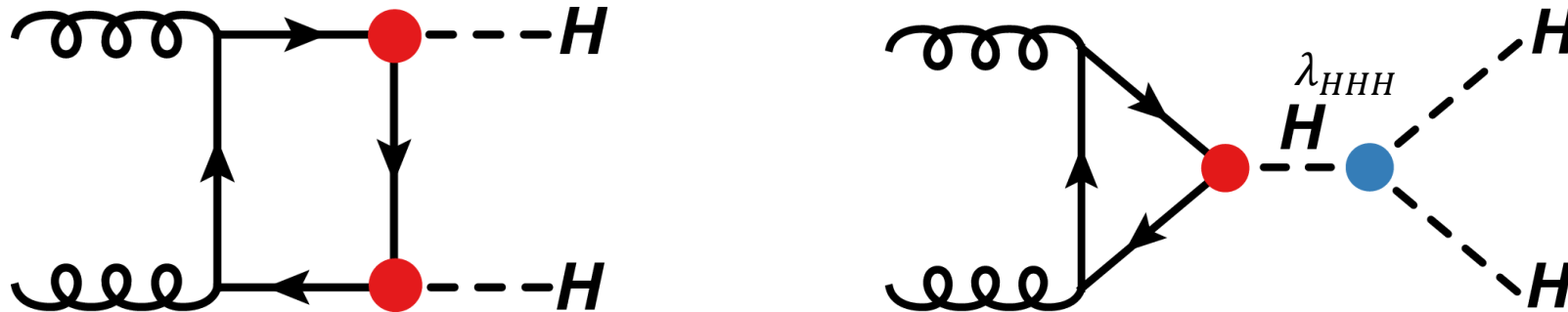
In all observed production modes, the Higgs boson is consistent with expectations.

Non-resonant Higgs boson pair production, however, has not yet been observed.



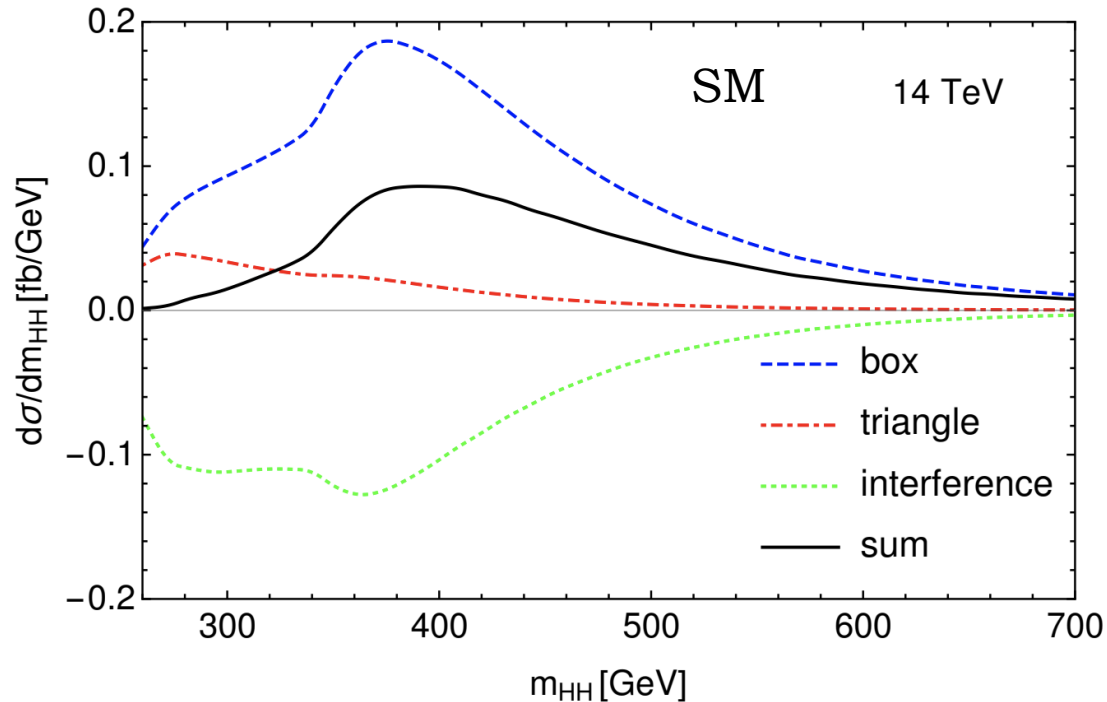
Higgs Pair-Production Cross Section

Most **searches for HH target gluon-fusion HH**, as it is the largest SM production mode.



Example diagrams that contribute to this process involve both top/bottom quark loops (“box” diagram) as well as those that involve the Higgs trilinear self-coupling.

Diagram Interference in SM



LHCHXSWG-2019-005

“Box” diagrams dominate the overall cross section, and a significant destructive interference occurs.

The SM cross section for ggF HH production is currently calculated as **31.05 ± 1.90 fb.**

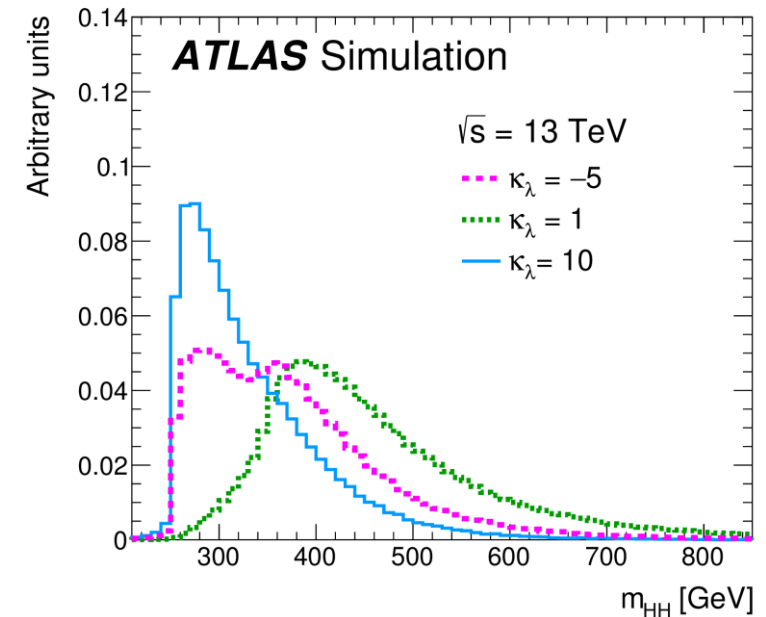
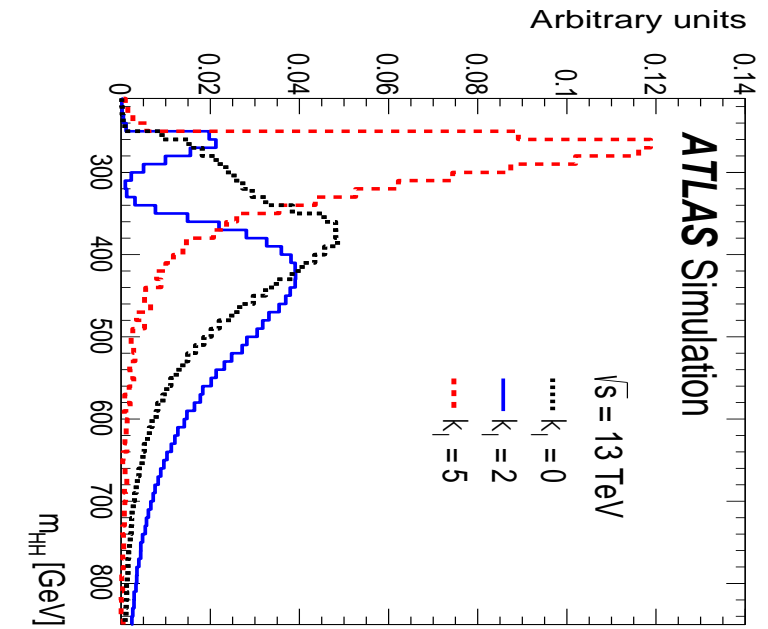
Looking **beyond the SM**, modifications to λ_{HHH} can affect the relative contribution of “box” and “triangle” diagrams.

Looking for New Physics

Searches for non-resonant HH thus set limits on two observables:

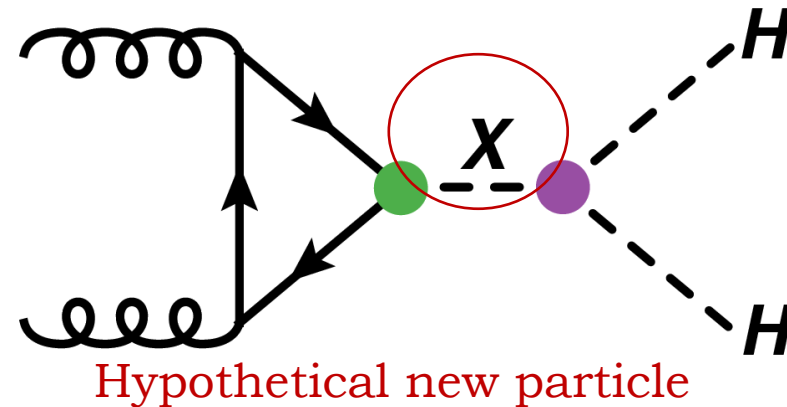
- **The overall HH production cross section**
 - Might be enhanced by new processes
 - Could be affected by new physics that affects λ_{HHH}
- **The trilinear Higgs boson self-coupling (λ_{HHH})**
 - Modifications are referred to as $\kappa_\lambda = \lambda/\lambda_{HHH}$.

Deviations in κ_λ affect both the **overall cross section** and the **kinematics** of signal events.



Di-Higgs in Resonant Searches

Another area to search for new physics is in resonant HH production:



This process involves a new, high mass particle that decays into two SM-like Higgs bosons.

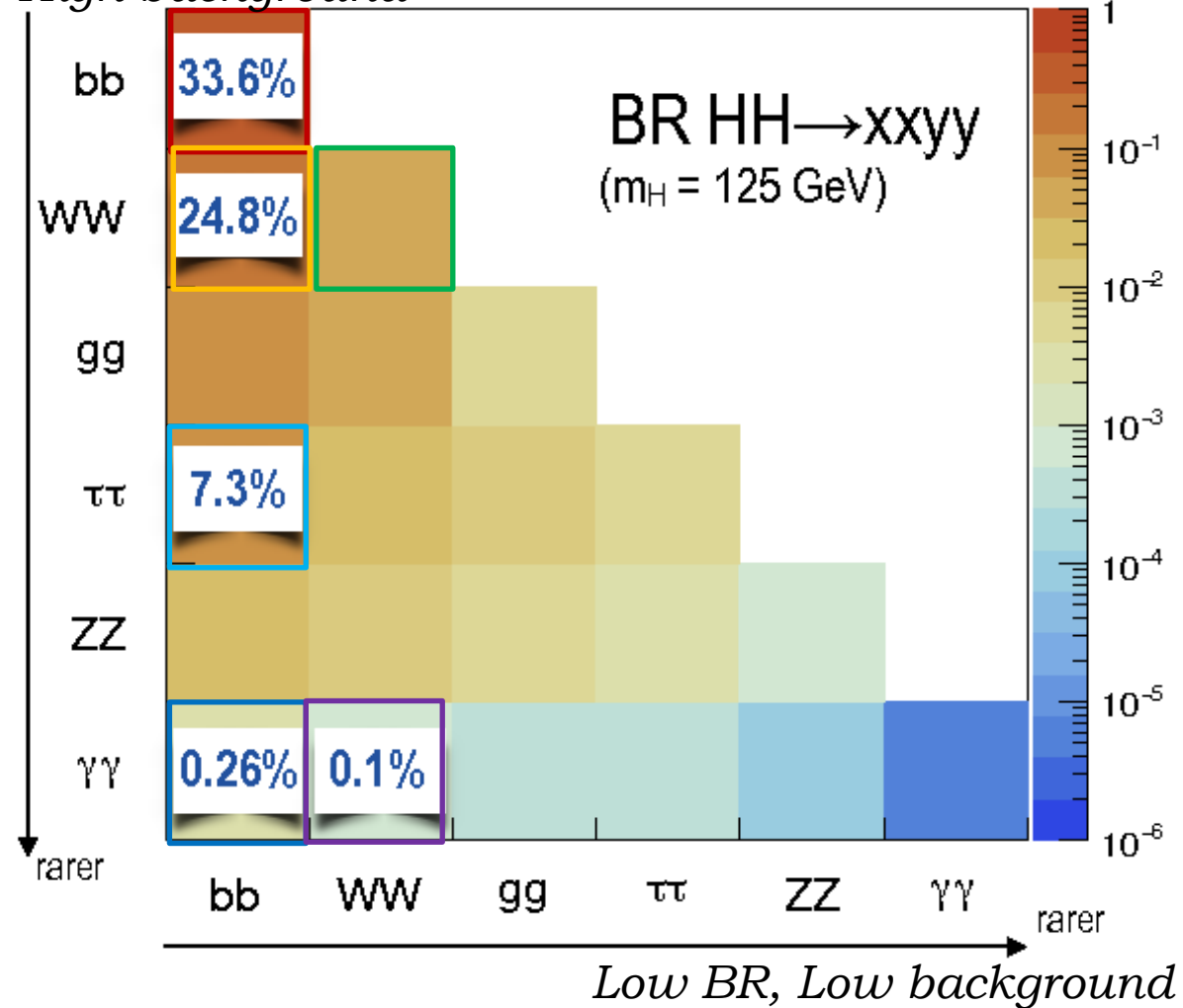
For these searches, the X mass range can be extended higher through the use of “boosted” techniques.

Searches for Di-Higgs

Summary of ATLAS approach to direct HH search

- For sensitivity, both **signal acceptance** and potential **background rejection** are important!
- bbbb**:
 - Resonant: Phys. Rev. D. 105, 092002
 - Non-resonant: ATLAS-CONF-2022-035
- bbWW***:
 - Dilepton: Phys. Lett. B 801 (2020) 135145
 - 1-lepton: JHEP 04 (2019) 092
- WW*WW***: JHEP 05 (2019) 12
- bb $\tau\tau$** :
 - Resolved: ATLAS-CONF-2021-030
 - Boosted: JHEP 11 (2020) 163
- $\gamma\gamma$ bb**: JHEP 11 (2018) 040
- $\gamma\gamma$ WW***: Eur. Phys. J. C 78 (2018) 1007

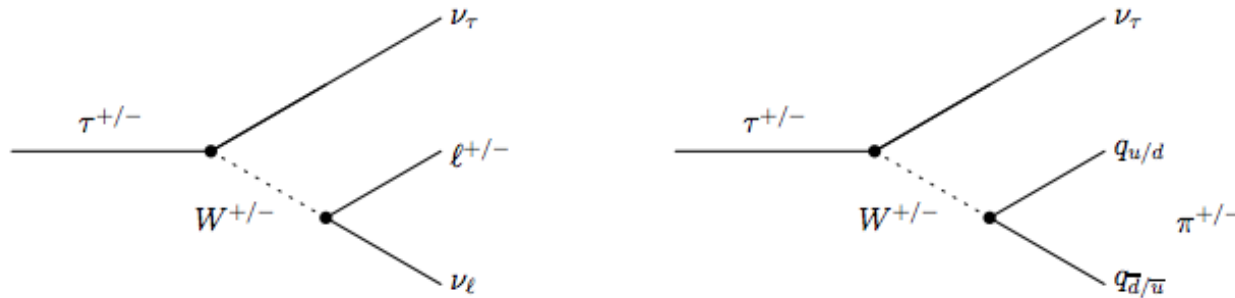
High BR,
High background



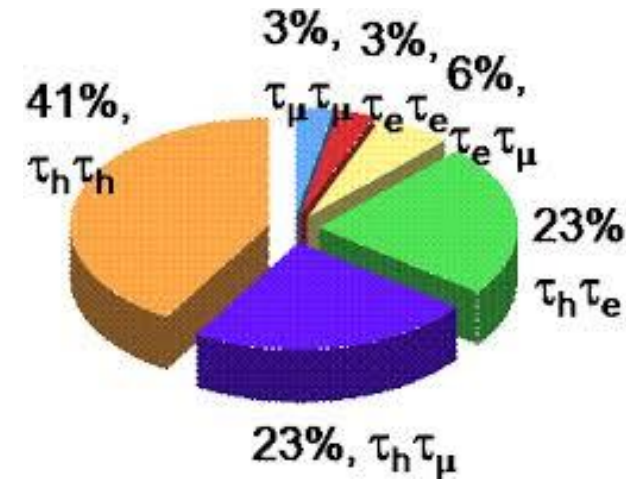
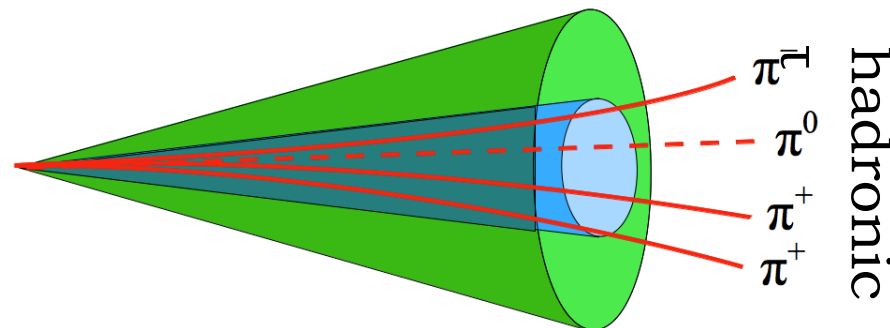
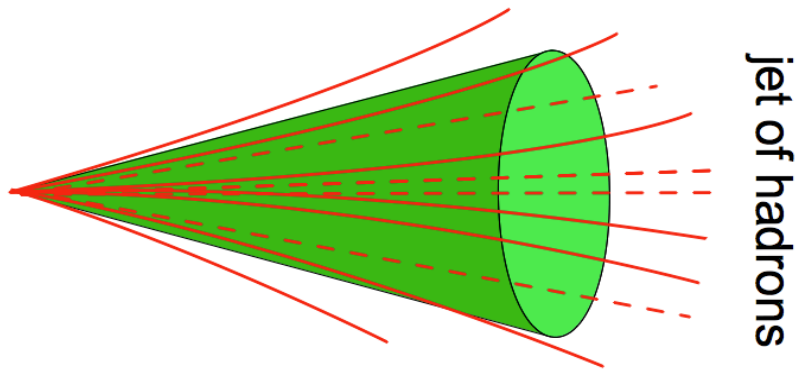
Several channels have also been combined (ATLAS-CONF-2021-052) to produce the strongest ATLAS HH result yet!

Brief Background on Tau Leptons

Due to their high mass, τ leptons can decay **leptonically or hadronically**.



Hadronic decays result in a signature **very similar to a hadronic jet**.



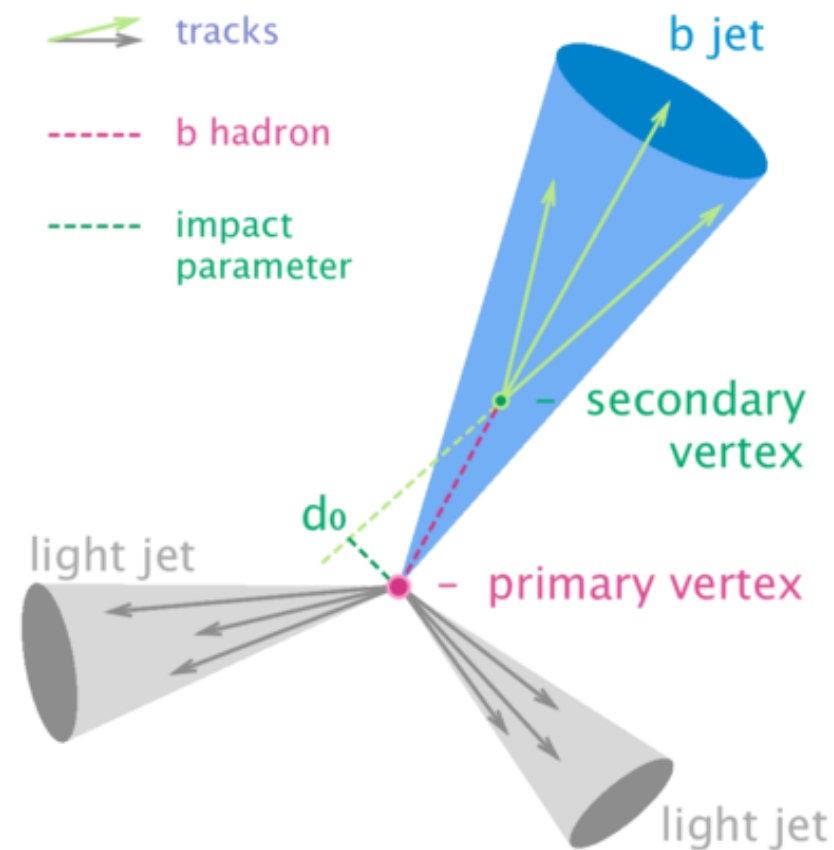
Having both leptonic and hadronic τ decays means there are multiple channels to consider for $b\bar{b}\tau\tau$: $\tau_{\text{had}}\tau_{\text{had}}$, $\tau_e\tau_{\text{had}}$, $\tau_\mu\tau_{\text{had}}$, $\tau_e\tau_e$, $\tau_\mu\tau_\mu$, $\tau_e\tau_\mu$

Brief Background on Bottom Quarks

b quarks produce a stream of particles that is identified by ATLAS as a **hadronic jet**.

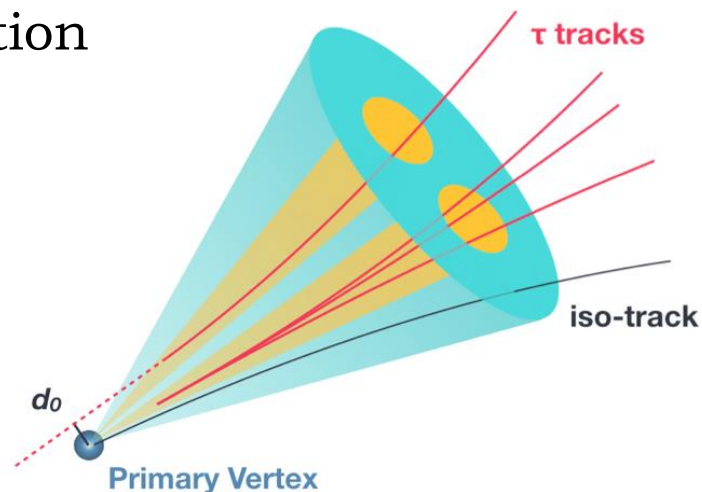
Machine learning techniques use differences to identify jets as “**b-tagged**”, as opposed to originating from a 1st/2nd generation quark (a ‘light jet’).

This classification is important for **physics that involves b quarks**.



Search for ggF $HH \rightarrow bb\tau\tau$

- **Resolved:** All four final state objects are distinguishable in the detector.
 - Channels with 1 τ decaying leptonically and 1 τ decaying hadronically ($\tau_{lep}\tau_{had}$) and with both τ decaying hadronically ($\tau_{had}\tau_{had}$)
 - Considering both **non-resonant** and **resonant** production
- **Boosted:** Some objects are highly collimated and indistinguishable in the detector.
 - Considering the channel with both τ decaying hadronically ($\tau_{had}\tau_{had}$)
 - Considering **resonant** production



Search for Boosted $HH \rightarrow b\bar{b}\tau\tau$

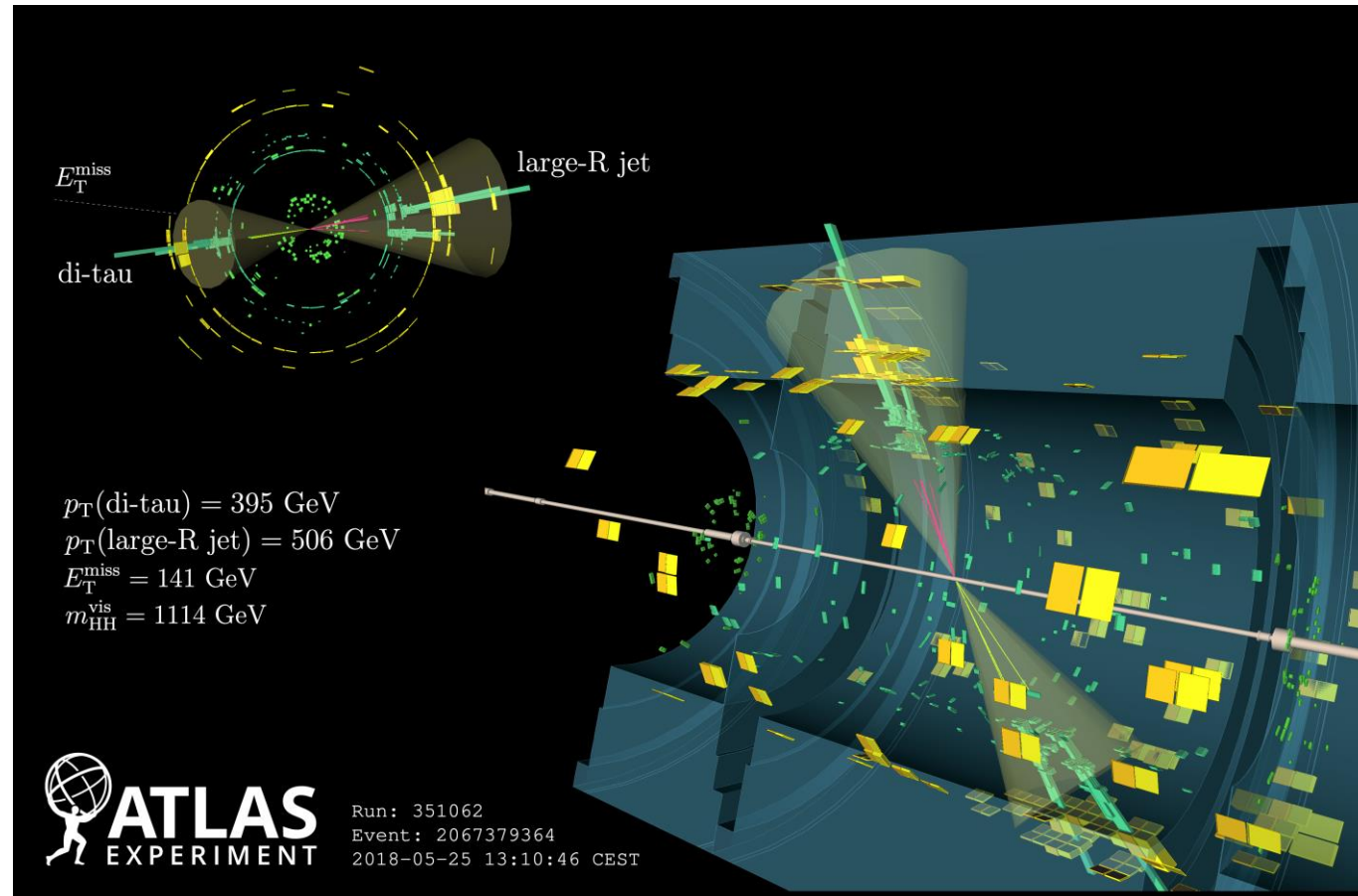
Targeting resonance masses of 1-3 TeV

In this range, both Higgs boson decay products become merged in the detector.

- ✓ Large-radius jets ($R = 1.0$, instead of standard $R = 0.4$) are used to capture the full decay products of each Higgs.

$H \rightarrow b\bar{b}$: $R=1.0$ jet with associated variable-radius track-jets ($R=0.02-0.4$) are checked with a multivariate b-tagging algorithm.

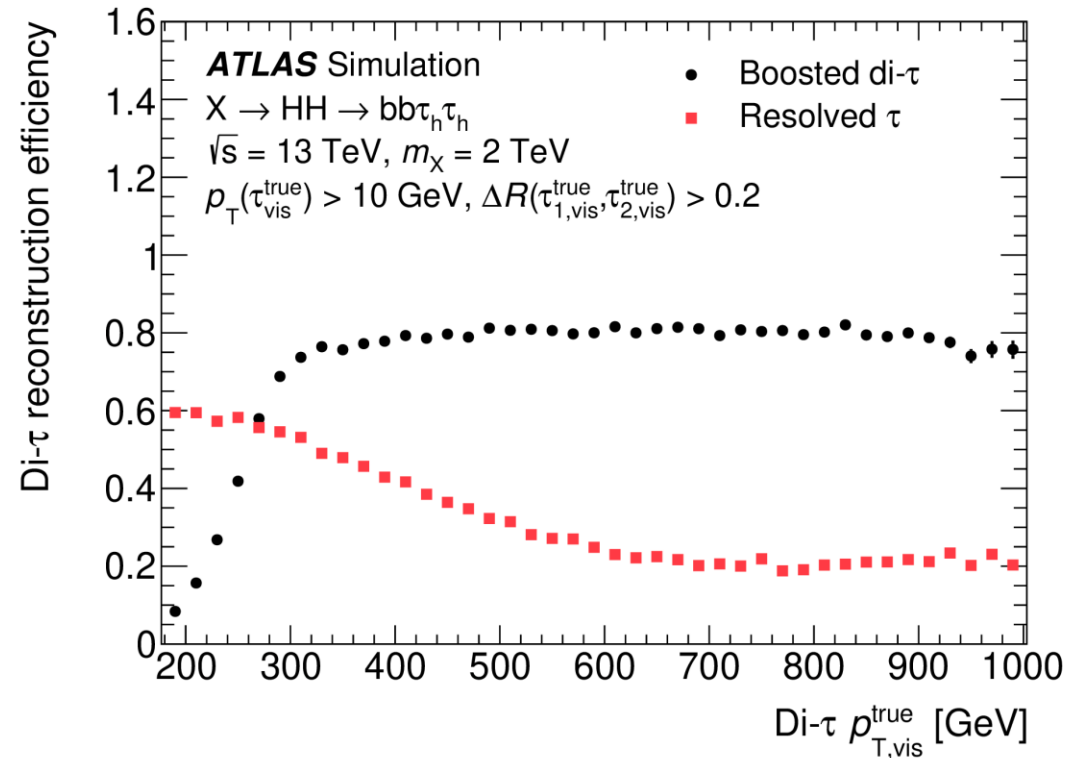
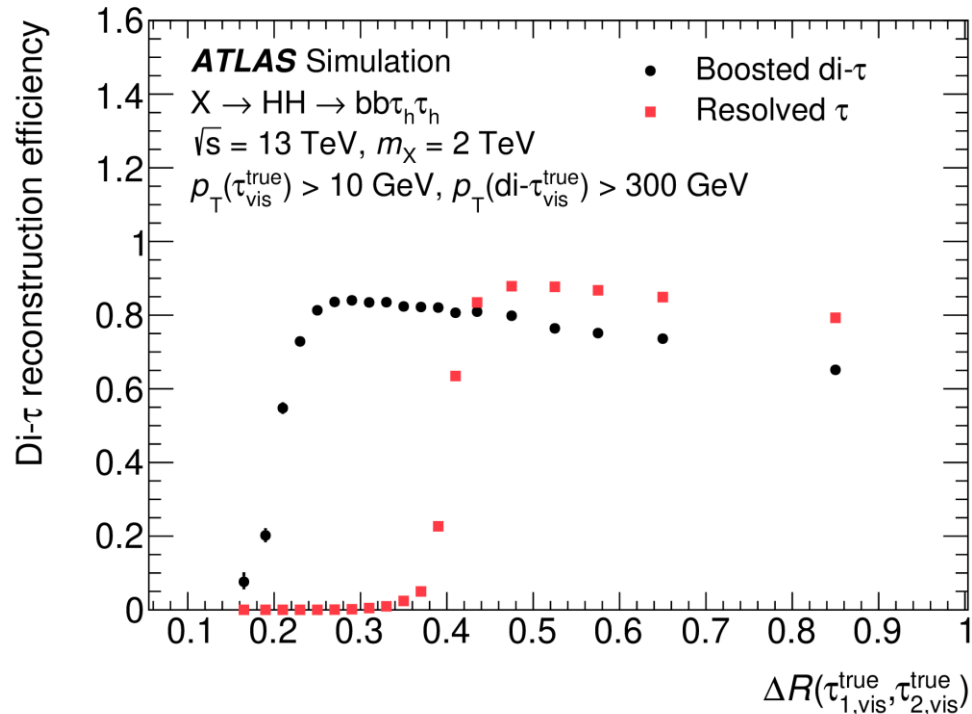
$H \rightarrow \tau_{had}\tau_{had}$: A new reconstruction and identification technique is developed and used in this analysis.



Reconstructing $H \rightarrow \tau_{had} \tau_{had}$

Reconstruction of di- τ objects requires:

- ✓ A large-R jet with $R=1.0$ and $P_T > 300$ GeV
- ✓ This jet contains at least 2 $R=0.2$ sub-jets with $P_T > 10$ GeV and at least 1 associated track.

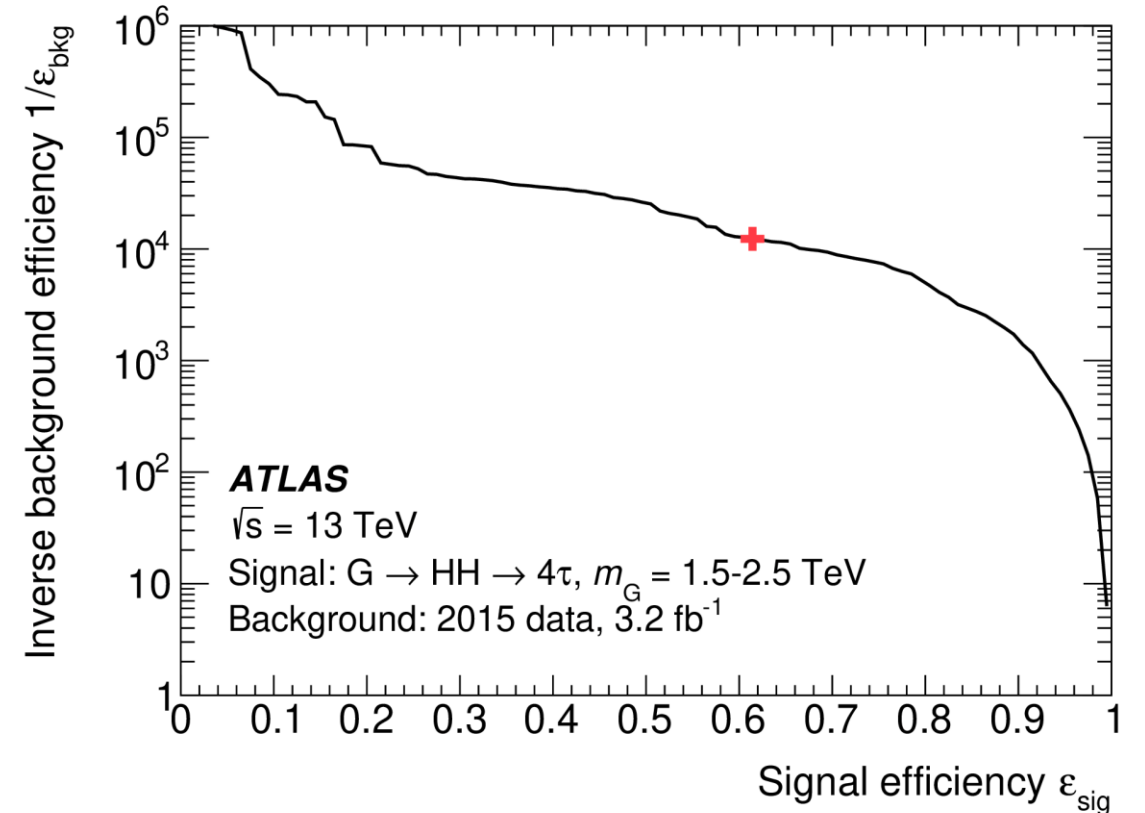
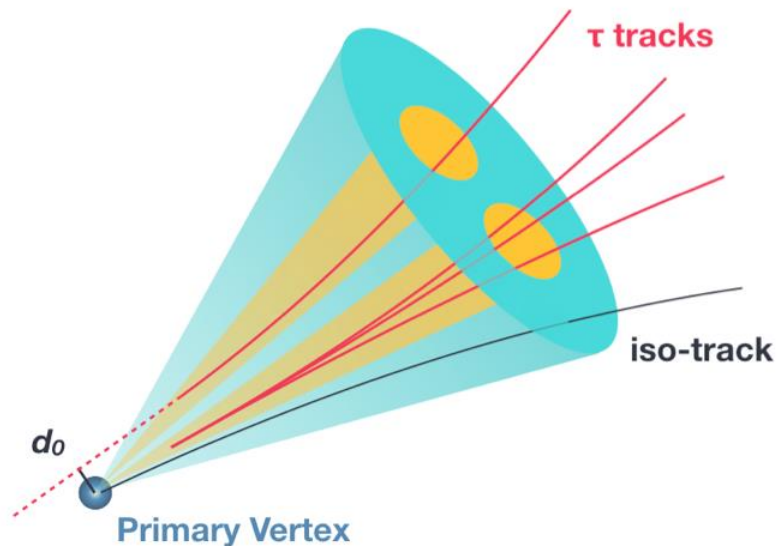


Efficiency of this reconstruction and standard tau reconstruction.

Identifying $H \rightarrow \tau_{had} \tau_{had}$

For the identification, a BDT is trained to select di- τ objects, trained against multi-jet events.

Variables used include information about clusters in the calorimeter, tracks, and vertices.



The Search for $X \rightarrow HH \rightarrow bb\tau_{had}\tau_{had}$

The boosted search uses this tagging technique, and a fake factor method to estimate the small multi-jet background.

Signal Region

1 di-tau object with:

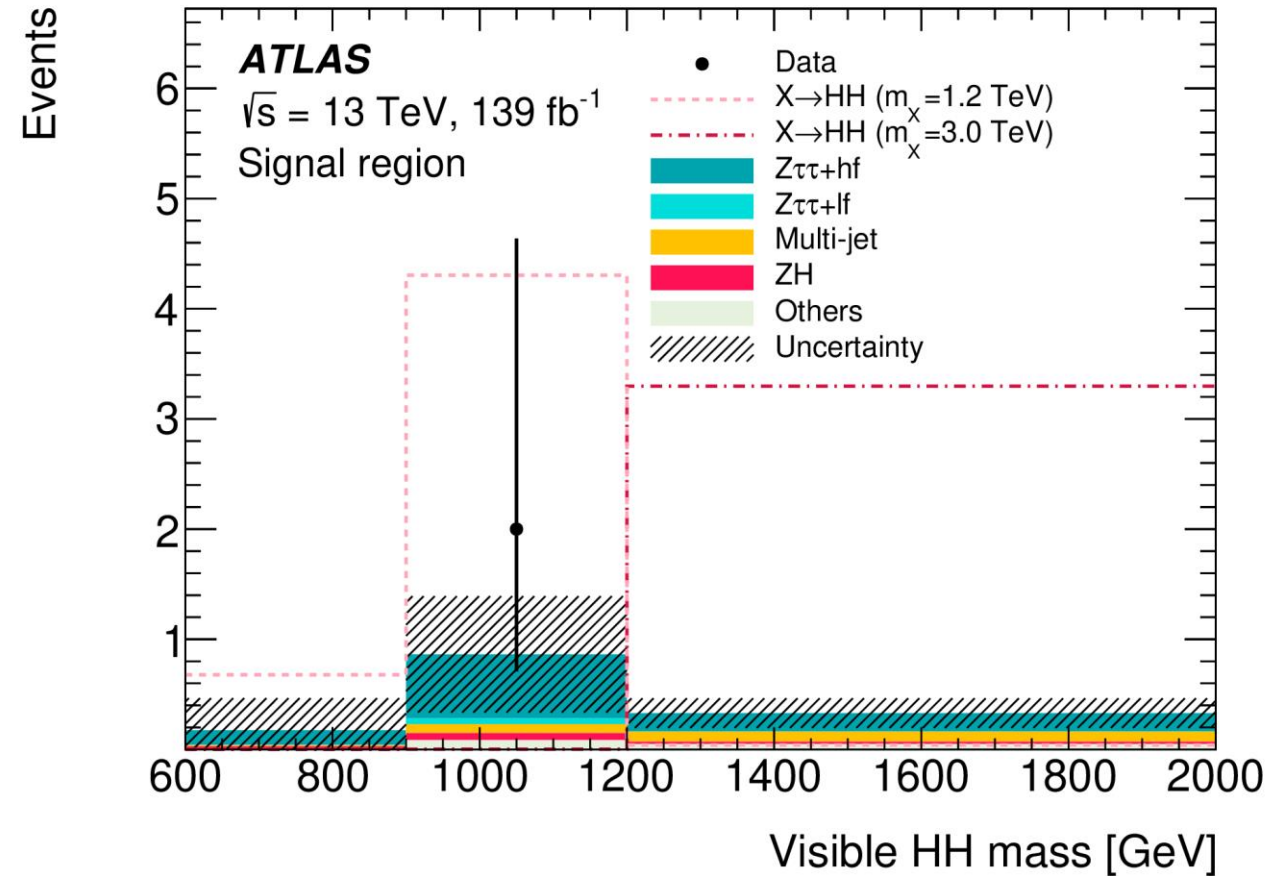
- 1-3 sub-jets
- $\Delta R < 0.8$ for 2 leading sub-jets
- $q^{lead} q^{sub-lead} = -1$

1 selected large-R jet with:

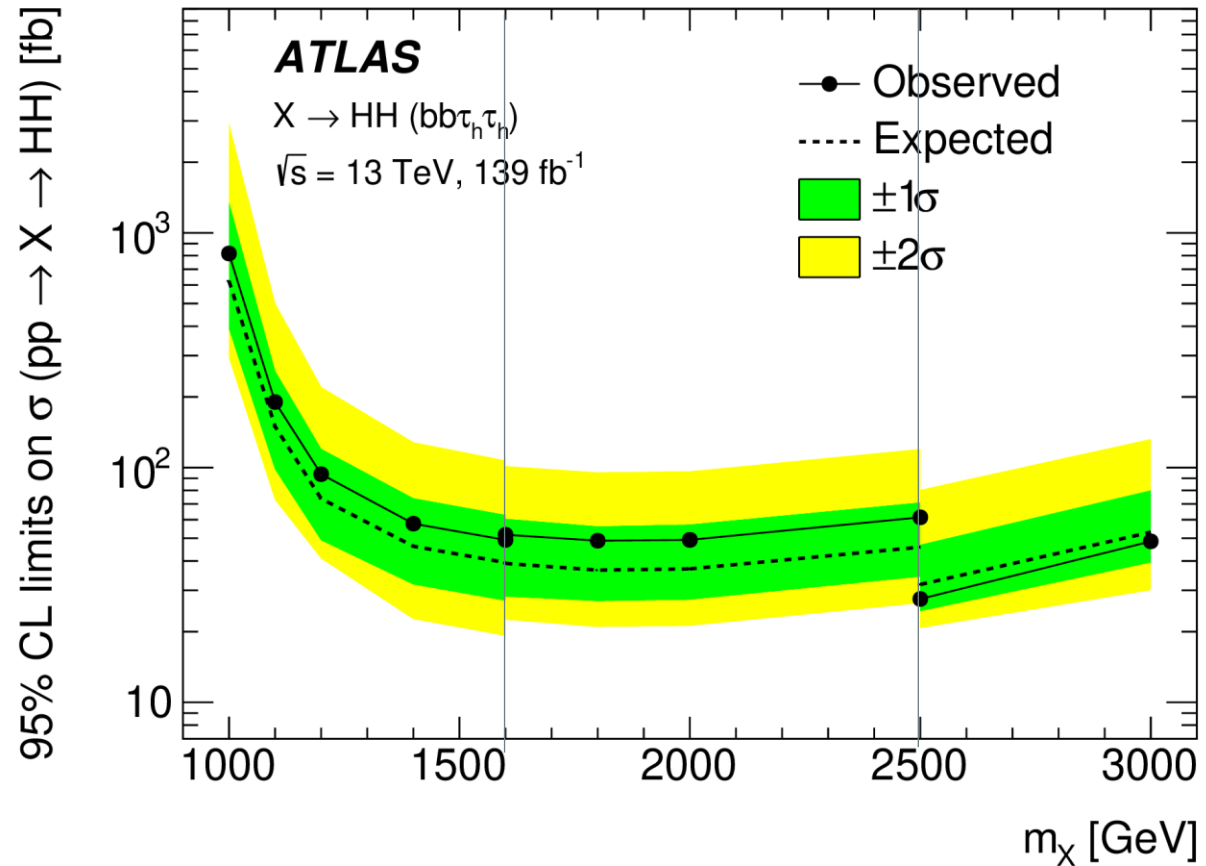
- 2 b-tagged track-jets
- $m_J = 60\text{--}160$ GeV

$$E_T^{\text{miss}} > 10 \text{ GeV and } |\Delta\phi_{di-\tau, MET}| < 1$$

$$M_{HH}^{\text{vis}} > 0, 900, 1200 \text{ GeV}$$



Results in the Search for $X \rightarrow HH \rightarrow bb\tau_{had}\tau_{had}$



Lines indicate where requirements on m_{HH}^{vis} are changed.

Resolved Search for $HH \rightarrow b\bar{b}\tau\tau$

Search covers $HH \rightarrow b\bar{b}\tau_{\text{had}}\tau_{\text{had(lep)}}$, m_X range 260-1000 GeV, final discriminant is a BDT

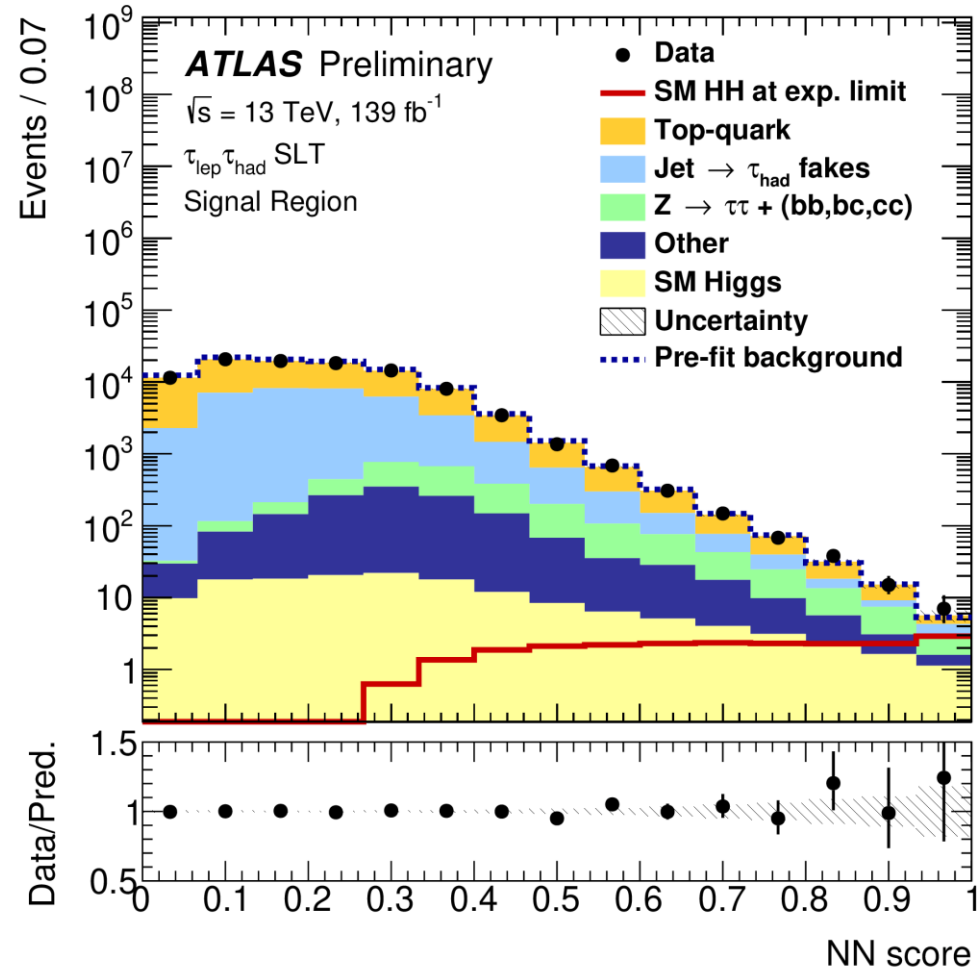
Signal scaled to expected limit.

Event Selection

- 1 e/μ and 1 τ_{had} , or 0 e/μ and 2 τ_{had}
- $m_{\tau\tau}^{\text{MMC}} > 60$ GeV
- 2 b-tagged jets

3 Signal Regions

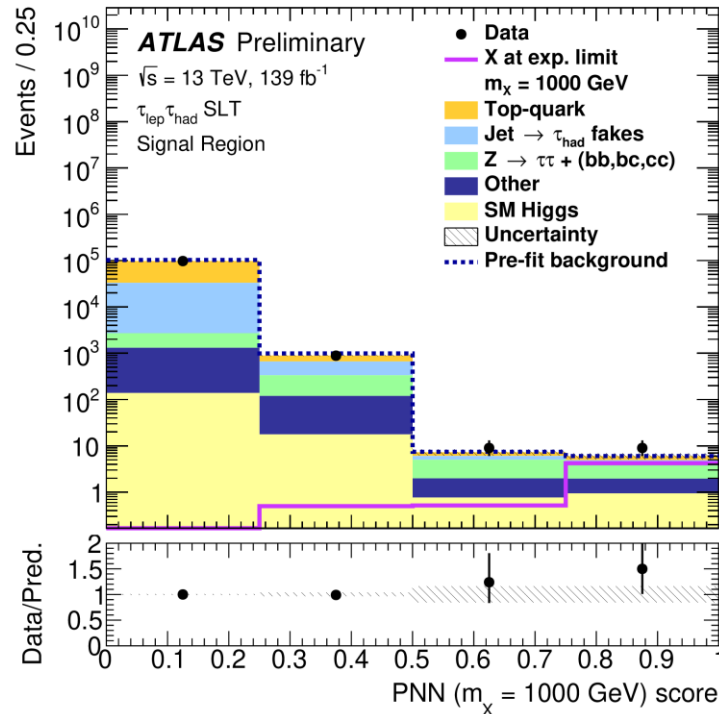
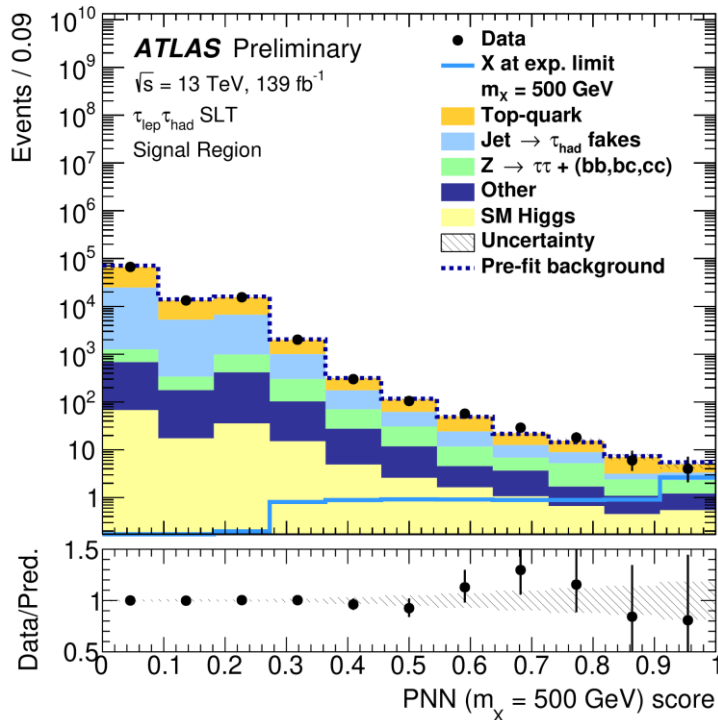
- **Single Lepton Trigger**
 - $p_T^{e/\mu} > 25\text{-}27$ GeV, $p_T^\tau > 20$ GeV, $p_T^{\text{jet,lead}} > 45$ GeV
- **Lepton+Tau Trigger**
 - $p_T^{e/\mu} > 18(15)$ GeV, $p_T^\tau > 30$ GeV, $p_T^{\text{jet,lead}} > 80$ GeV
- **Single(Di)-Tau Trigger**
 - $p_T^{\tau,\text{lead}} > 40\text{-}180$ GeV, $p_T^{\tau,\text{sublead}} > 20$ (30) GeV, $p_T^{\text{jet,lead}} > 45$ (80) GeV



Resolved Search for $HH \rightarrow b\bar{b}\tau\tau$

A parametric neural network was designed, taking mass as a parameter for the resonant case.

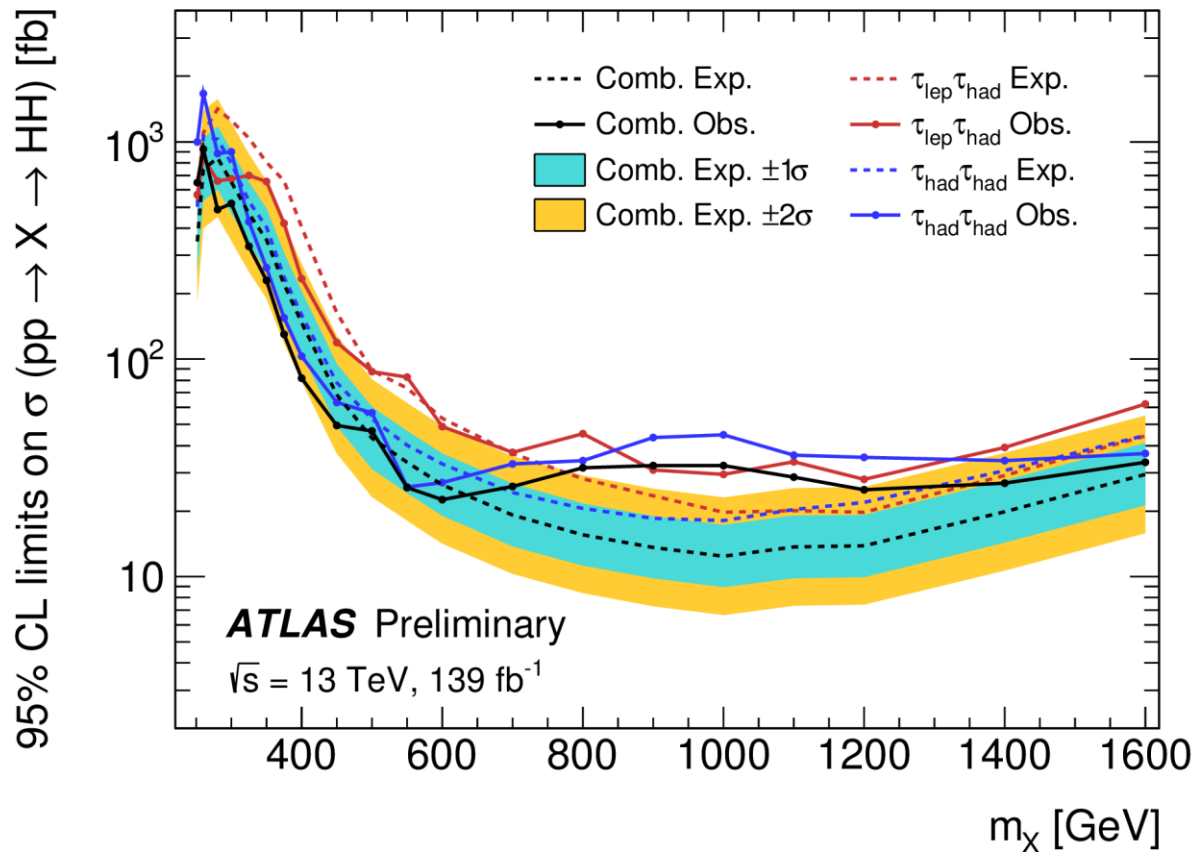
- Neural networks take advantage of small differences in shape between signal and background in multiple variables.
- The NN creates an output ‘score’ that describes how background-like (left) or signal-like (right) an event is.



Signal scaled to expected limit.

Variable	$\tau_{\text{had}}\tau_{\text{had}}$	$\tau_{\text{lep}}\tau_{\text{had}}$	SLT	LTT
m_{HH}	✓		✓	✓
$m_{\tau\tau}^{\text{MMC}}$	✓		✓	✓
m_{bb}	✓		✓	✓
$\Delta R(\tau, \tau)$	✓		✓	✓
$\Delta R(b, b)$	✓		✓	
$\Delta p_T(\ell, \tau)$			✓	✓
Sub-leading b -tagged jet p_T			✓	
m_T^W			✓	
E_T^{miss}			✓	
p_T^{miss} ϕ centrality			✓	
$\Delta\phi(\tau\tau, bb)$			✓	
$\Delta\phi(\ell, p_T^{\text{miss}})$				✓
$\Delta\phi(\ell\tau, p_T^{\text{miss}})$				✓
S_T				✓

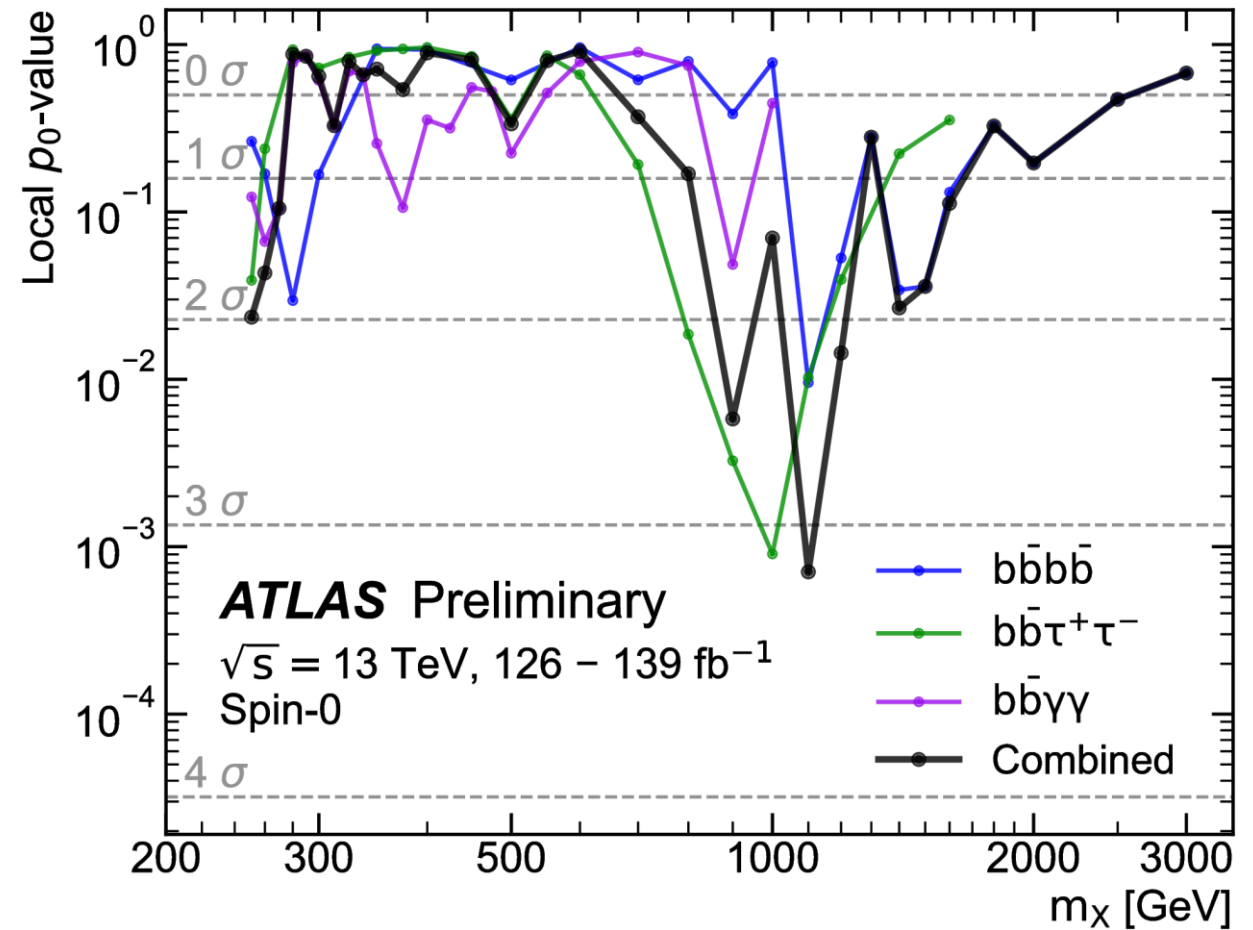
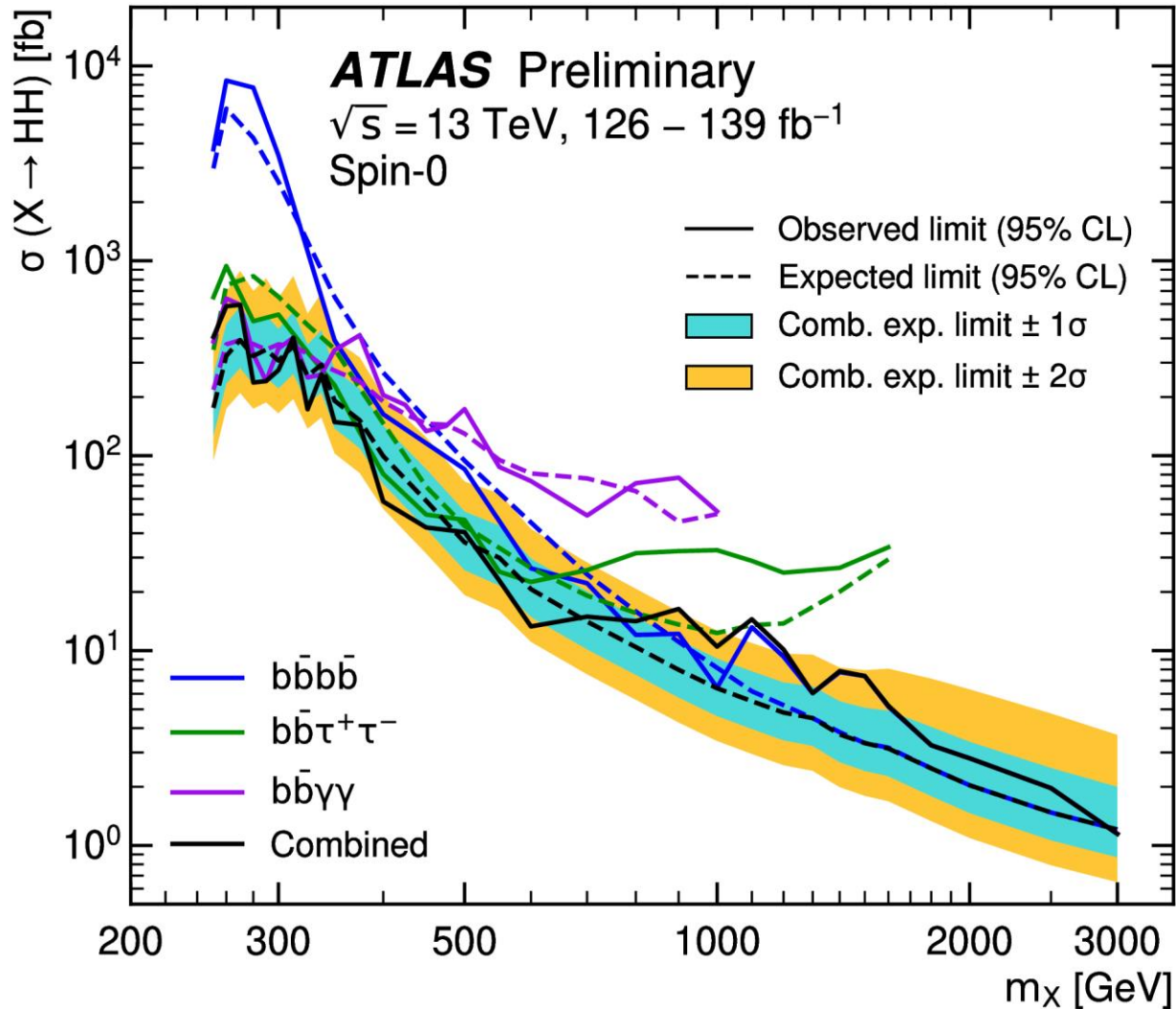
Resonant Results



- Excess is seen near 1 TeV! Almost a year was spent fully studying and checking the statistical strength of this excess.
 - e.g. how likely is it that we would get a statistical fluctuation in data that would cause this?
- Looking only at the point with the largest deviation, we see a 3σ excess. However, we also consider the “look-elsewhere effect”.
- The look-elsewhere effect is **a phenomenon in the statistical analysis of scientific experiments where an apparently statistically significant observation may have actually arisen by chance because of the sheer size of the parameter space to be searched.**
- When we take this into account, we find that the “global significance” of the excess is 2σ .
- This is *interesting*, but not yet evidence of something new.

Di-Higgs Combination

Resonant



- Excess is not inconsistent with other channels – potentially more interesting!

Non-Resonant Results

Remember, the two targets for the non-resonant case are:

1. The total **production cross section**
2. The value of the Higgs **trilinear self-coupling** relative to the expected SM value ($\kappa_\lambda = \frac{\lambda_{hhh}}{\lambda_{SM}}$)

Below are shown the exclusions for the cross section, for the $bb\tau\tau$ channels, both separately and combined.

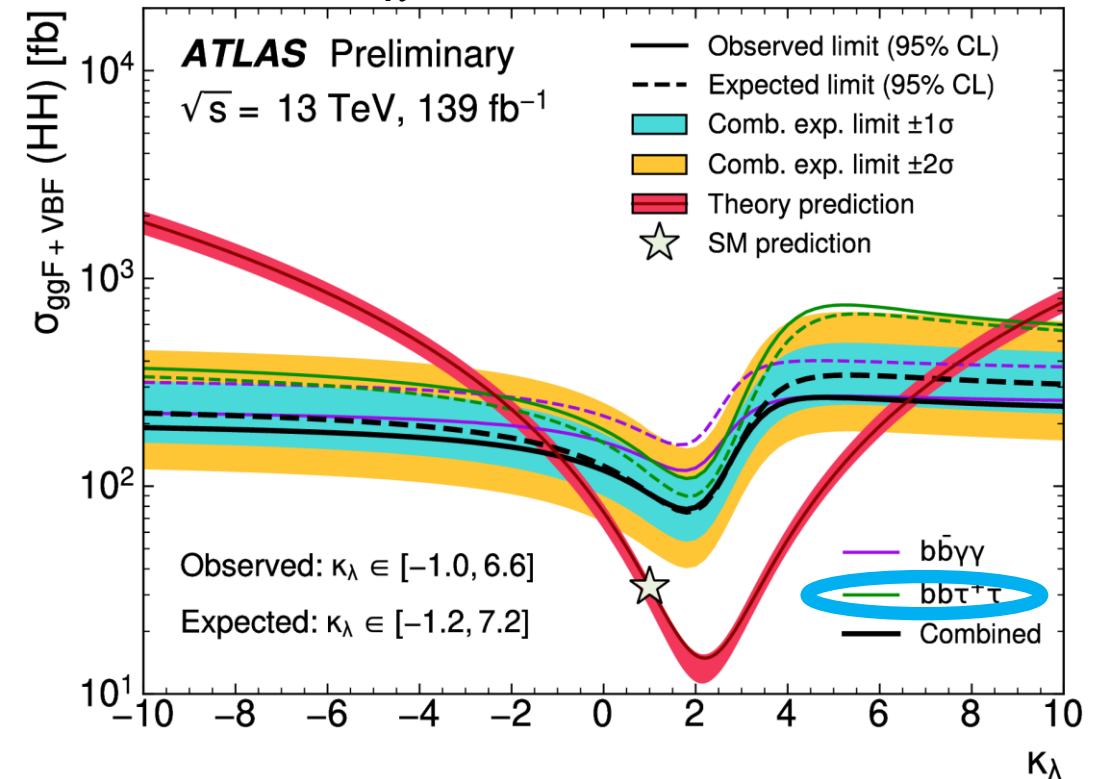
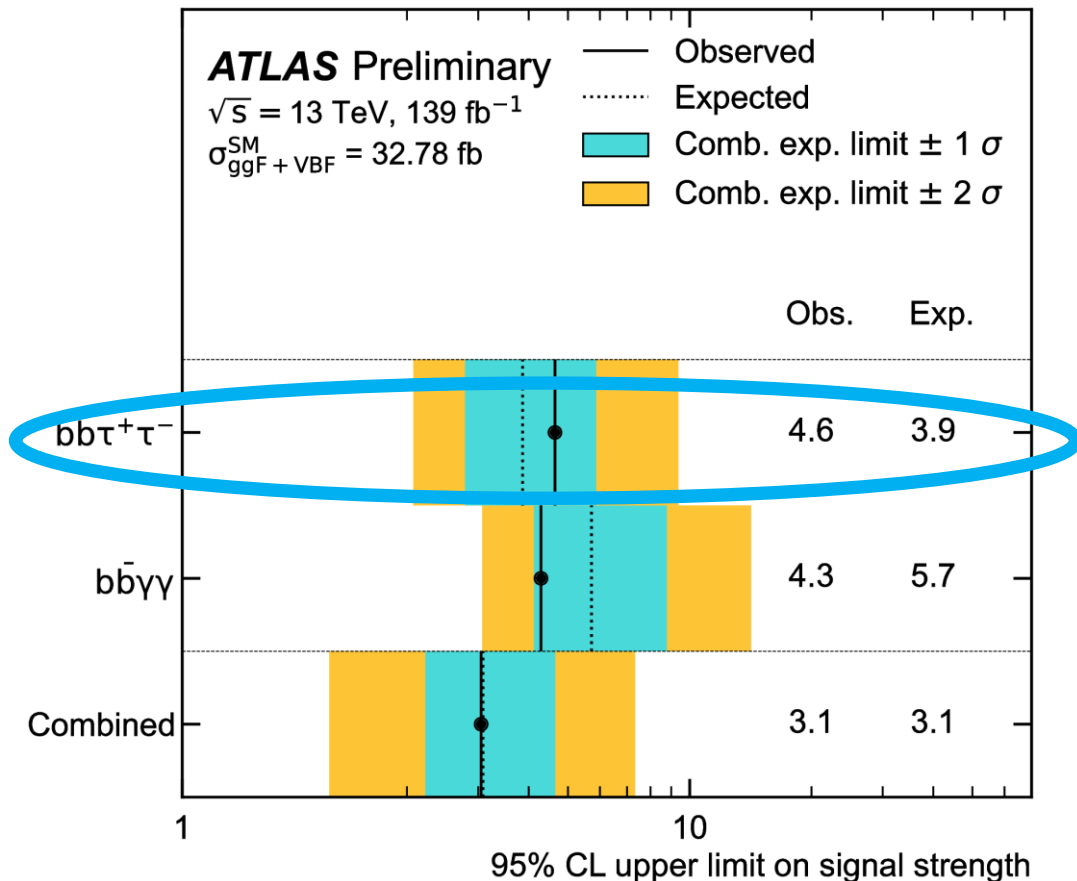
		Observed	-2σ	-1σ	Expected	$+1 \sigma$	$+2 \sigma$
$\tau_{\text{had}}\tau_{\text{had}}$	$\sigma_{\text{ggF+VBF}}$ [fb]	145	70.5	94.6	131	183	245
	$\sigma_{\text{ggF+VBF}}/\sigma_{\text{ggF+VBF}}^{\text{SM}}$	4.95	2.38	3.19	4.43	6.17	8.27
$\tau_{\text{lep}}\tau_{\text{had}}$	$\sigma_{\text{ggF+VBF}}$ [fb]	265	124	167	231	322	432
	$\sigma_{\text{ggF+VBF}}/\sigma_{\text{ggF+VBF}}^{\text{SM}}$	9.16	4.22	5.66	7.86	10.9	14.7
Combined	$\sigma_{\text{ggF+VBF}}$ [fb]	135	61.3	82.3	114	159	213
	$\sigma_{\text{ggF+VBF}}/\sigma_{\text{ggF+VBF}}^{\text{SM}}$	4.65	2.08	2.79	3.87	5.39	7.22

Di-Higgs Combination Non-Resonant

Here the $bb\tau\tau$ channel is shown in comparison and combination with another HH channel:

Left: for the overall constraints on the non-resonant cross section relative to the SM.

Right: for the limit on the cross section for a range of values of κ_λ .



Observed (Expected) exclusion of
 $-5.0(-5.8) < \kappa_\lambda < 12.0(12.0)$

Conclusions

- I have shown today some of the **strategies** used in the search for unobserved processes and/or new physics.
- **Higgs boson pair-production**, while interesting in the Standard Model, also provides a path for discovery in the **search for new physics**.
- **New ideas are quickly progressing**: machine learning techniques, combination with single Higgs boson measurements, boosted techniques and more.
- Looking forward to Run-3 with more data and new ideas!

Backup

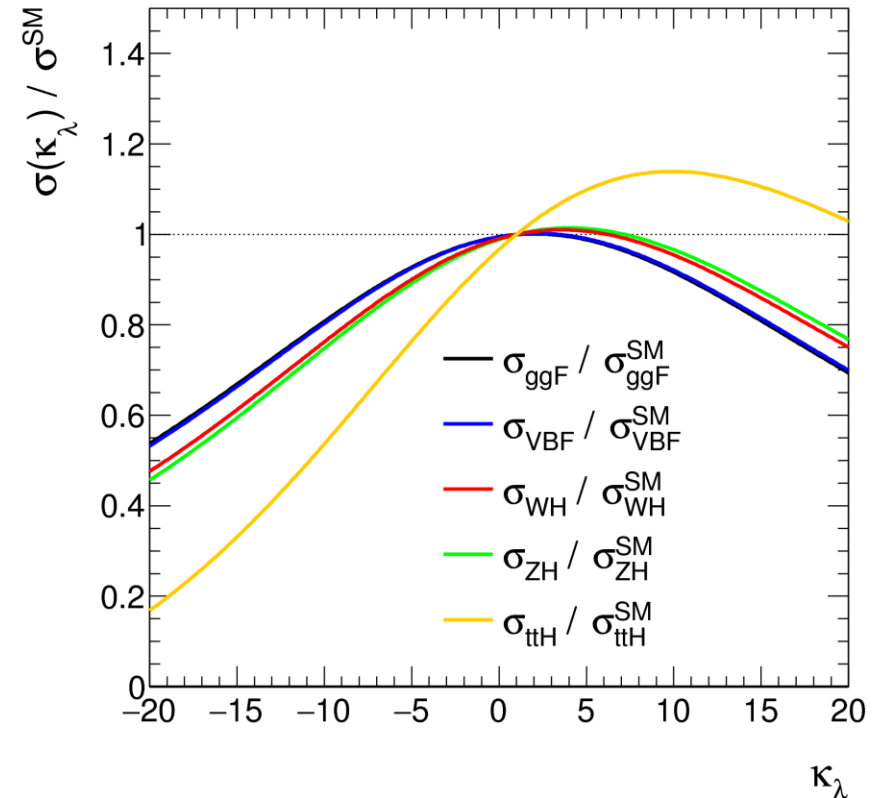
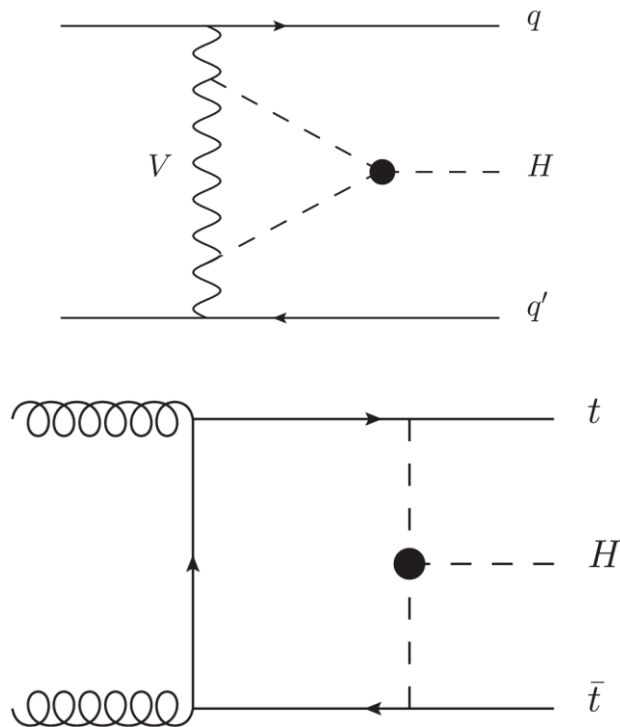
Di-Higgs + Single Higgs Combination

Non-resonant

At one-loop level, there is an impact on single Higgs production from the Higgs trilinear self-coupling.

This represents a source of information complementary to direct searches for HH.

Example diagrams



Di-Higgs + Single Higgs Combination

Non-resonant

If you consider both H and HH results, a global fit can be performed without the assumption that only the trilinear self-coupling changes with new physics.

Model	$\kappa_W^{+1\sigma}_{-1\sigma}$	$\kappa_Z^{+1\sigma}_{-1\sigma}$	$\kappa_t^{+1\sigma}_{-1\sigma}$	$\kappa_b^{+1\sigma}_{-1\sigma}$	$\kappa_\ell^{+1\sigma}_{-1\sigma}$	$\kappa_\lambda^{+1\sigma}_{-1\sigma}$	κ_λ [95% CL]	
κ_λ -only	1	1	1	1	1	$4.6^{+3.2}_{-3.8}$	[-2.3, 10.3]	obs.
						$1.0^{+7.3}_{-3.8}$	[-5.1, 11.2]	exp.
Generic	$1.03^{+0.08}_{-0.08}$	$1.10^{+0.09}_{-0.09}$	$1.00^{+0.12}_{-0.11}$	$1.03^{+0.20}_{-0.18}$	$1.06^{+0.16}_{-0.16}$	$5.5^{+3.5}_{-5.2}$	[-3.7, 11.5]	obs.
	$1.00^{+0.08}_{-0.08}$	$1.00^{+0.08}_{-0.08}$	$1.00^{+0.12}_{-0.12}$	$1.00^{+0.21}_{-0.19}$	$1.00^{+0.16}_{-0.15}$	$1.0^{+7.6}_{-4.5}$	[-6.2, 11.6]	exp.

This is the strongest result yet, and highlights the gains to be had through collaboration between the H and HH teams.

Higgs Pair-Production in the Standard Model

First, let's consider Higgs pair-production in the Standard Model:

Starting with the Higgs potential:

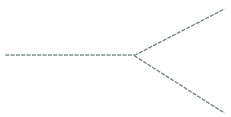
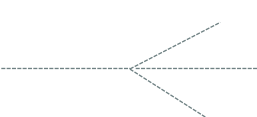
$$V(\varphi) = -\mu^2\varphi + \lambda\varphi^4$$

We can expand it about the minimum ($\varphi \rightarrow v + h$), with $v = \mu/\sqrt{\lambda}$

$$V(h) = V_0 + \lambda v^2 h^2 + \lambda v h^3 + \frac{\lambda}{4} h^4$$

↓

$$V(h) = V_0 + \underbrace{\frac{1}{2} m_h^2 h^2}_{\text{Higgs mass term}} + \underbrace{\frac{m_h^2}{2v^2} v h^3}_{\text{HH term}} + \underbrace{\frac{1}{24} \frac{m_h^2}{v^2} h^4}_{\text{HHH term}}$$

Di- τ Tagger Calibration

Scale factors to correct the performance in simulation relative to data and associated uncertainties are evaluated in a $Z \rightarrow \tau\tau$ control region.

Control Region

1 di-tau object with:

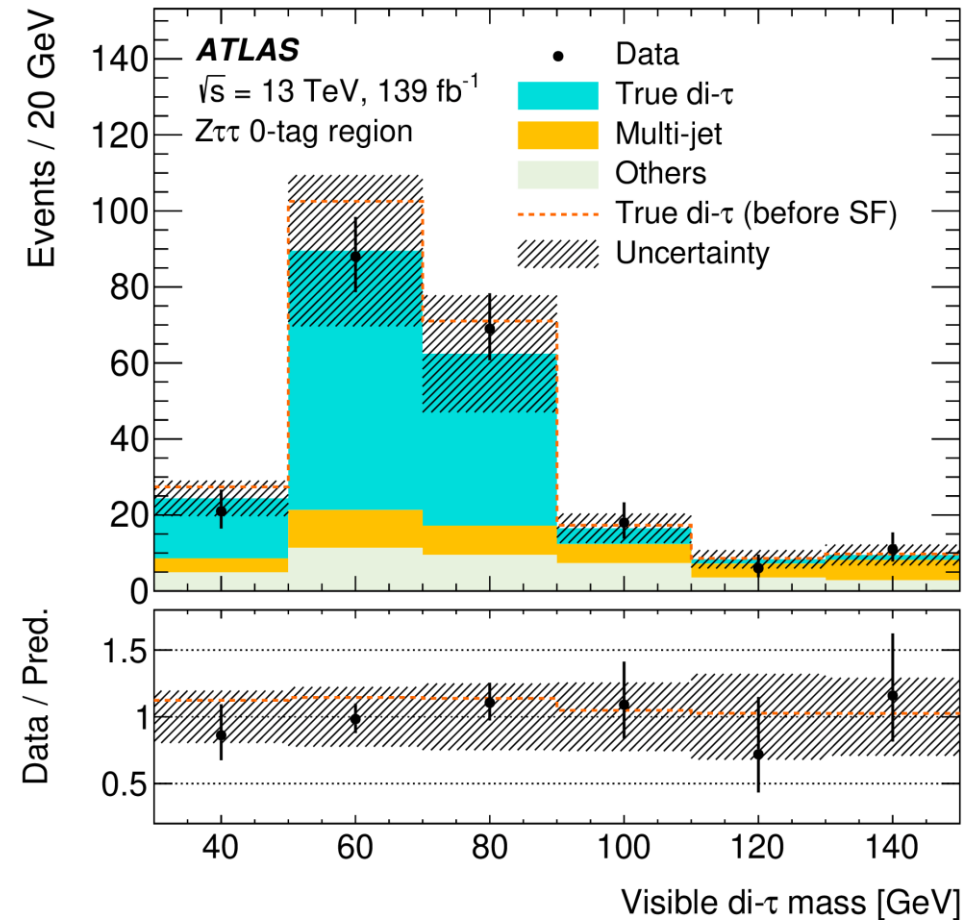
- 1-3 sub-jets
- $\Delta R < 0.8$ for 2 leading sub-jets
- $q^{lead} q^{sub-lead} = -1$

1 selected large-R jet with:

- no b-tagged track-jets

$E_T^{miss} > 10$ GeV and $|\Delta\phi_{di-\tau, MET}| < 1$

$$SF = \frac{N(\text{data}) - N(\text{non-di-}\tau)}{N(\text{true di-}\tau)} = 0.84 \pm 0.09 \text{ (stat)} \begin{matrix} +0.14 \\ -0.13 \end{matrix} \text{ (Z-modelling)} \begin{matrix} +0.19 \\ -0.20 \end{matrix} \text{ (syst).}$$



Data-driven Techniques in $\tau_{\text{lep}}\tau_{\text{had}}$: Jet- \rightarrow τ Backgrounds

$$\text{Combined Fake Factor} = \text{FF}_{\text{t\bar{t}}} (1 - r_{\text{QCD}}) + \text{FF}_{\text{QCD}} r_{\text{QCD}}$$

The tables below show how each piece of the equation is derived.

		τ failing selection	τ passing selection
Isolated Lepton		Anti-tau Control Region	Signal Region
Anti-Isolated Lepton		FF_{QCD} denominator (data- true tau)	FF_{QCD} numerator (data- true tau)

r_{QCD} is close to 0 for the 2 b-tag region, and it is determined using simulation.



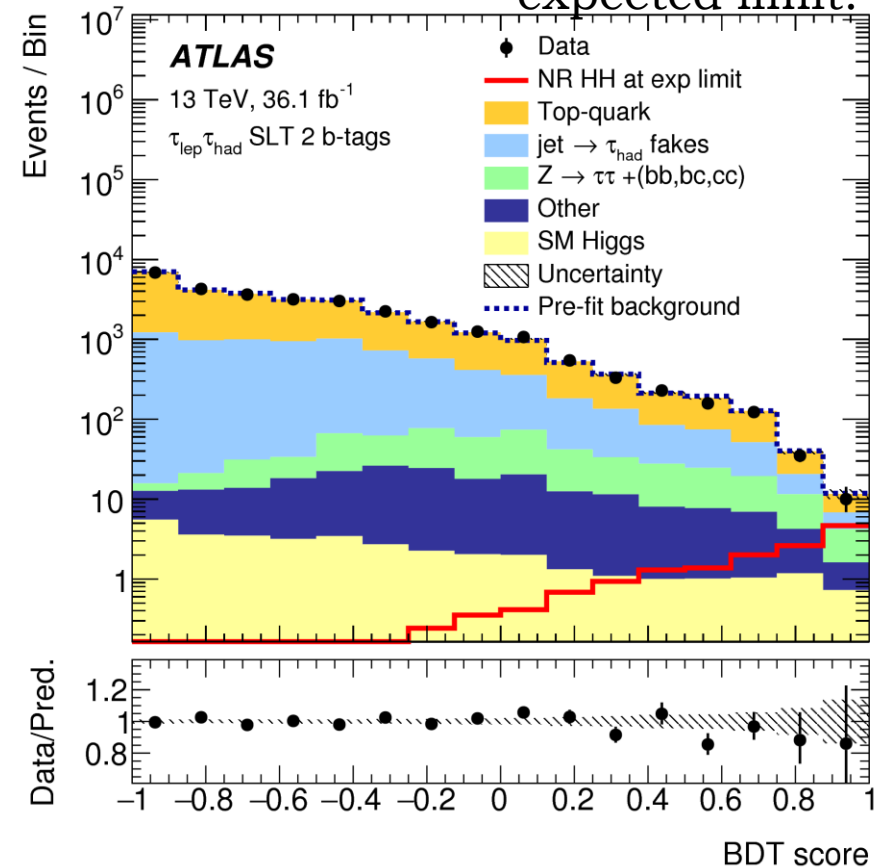
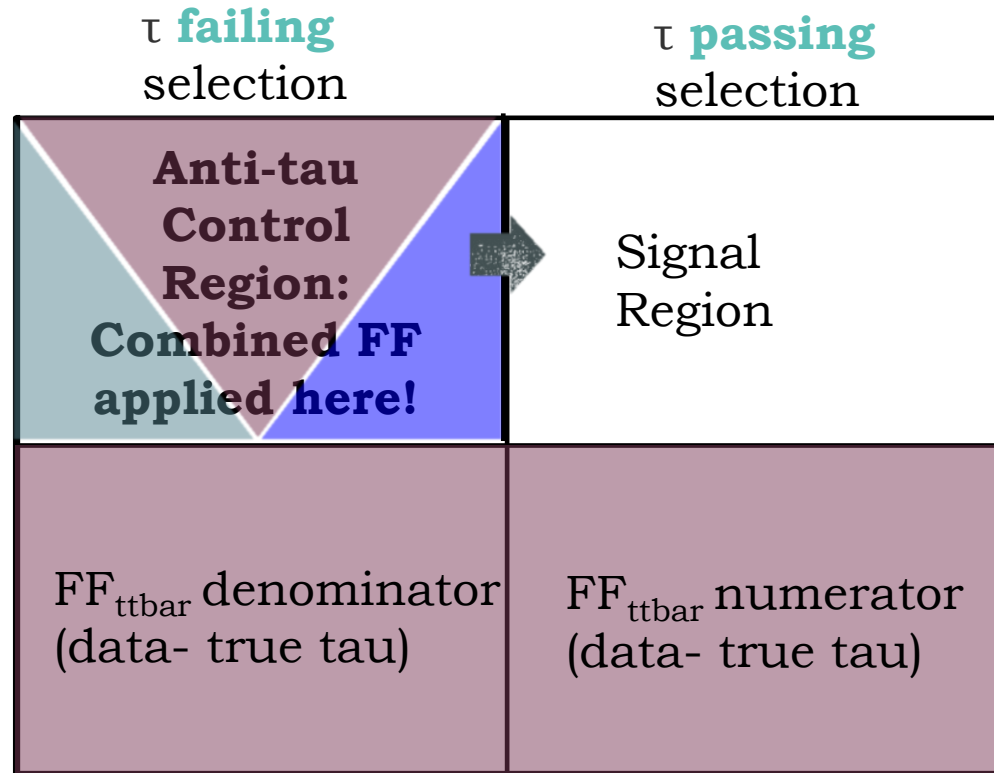
Data-driven Techniques in $\tau_{\text{lep}}\tau_{\text{had}}$: Jet- \rightarrow τ Backgrounds

$$\text{Combined Fake Factor} = \text{FF}_{\text{ttbar}}(1-r_{\text{QCD}}) + \text{FF}_{\text{QCD}}r_{\text{QCD}}$$

The tables below show how each piece of the equation is derived.

Signal scaled to expected limit.

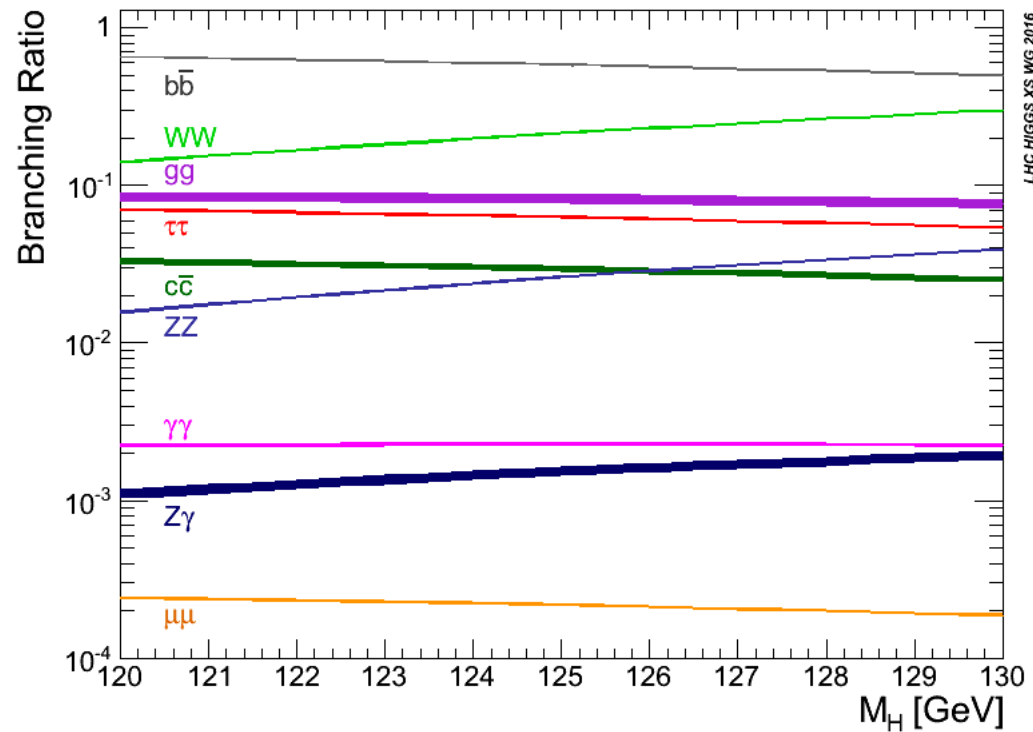
All Leptons are isolated.



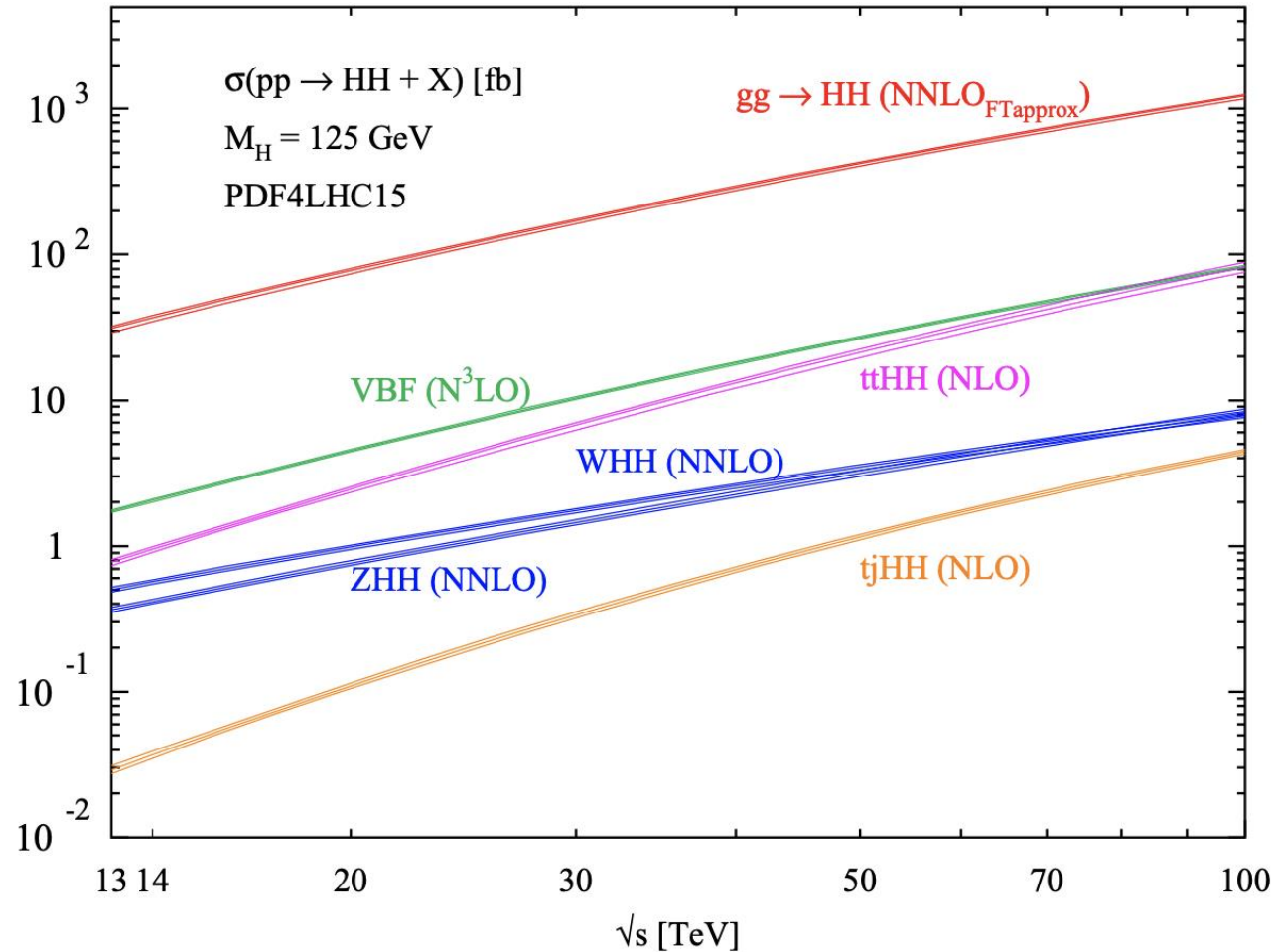
The ttbar CR is defined by $M_T^W(\text{lepton}, E_T^{\text{miss}}) > 40 \text{ GeV}$.



SM Higgs Boson Branching Ratios



Higgs Pair-Production in the Standard Model



Variables used in Boosted di-tau BDT

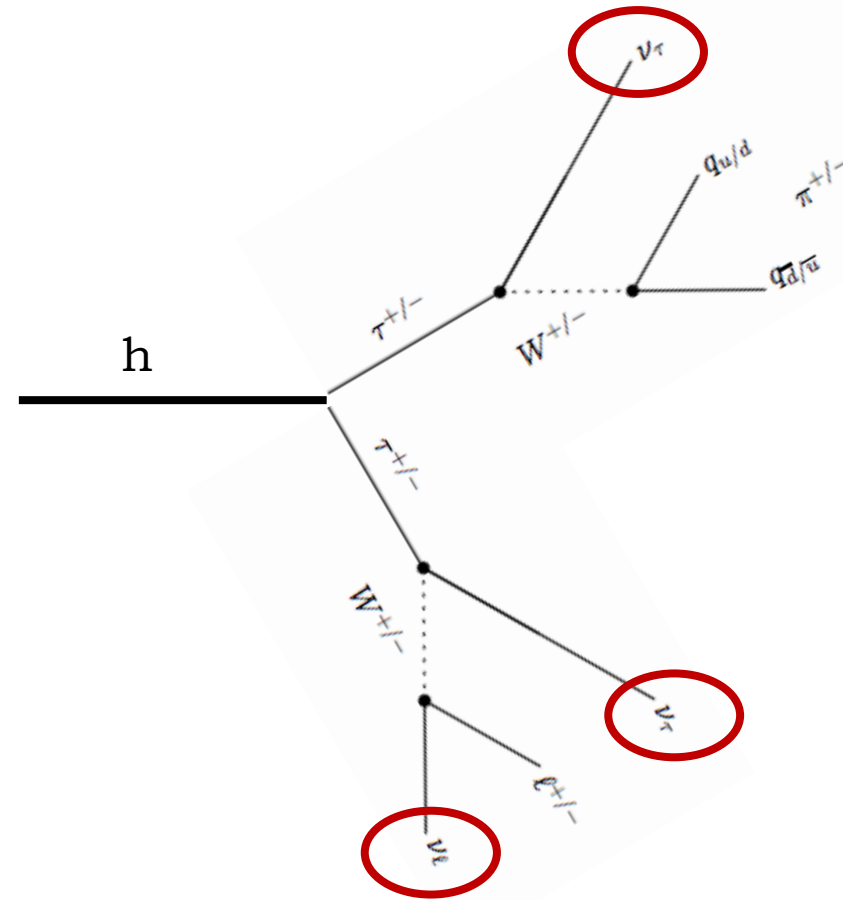
Variable	Definition
$E_{\Delta R < 0.1}^{sj_1} / E_{\Delta R < 0.2}^{sj_1}$ and $E_{\Delta R < 0.1}^{sj_2} / E_{\Delta R < 0.2}^{sj_2}$	Ratios of the energy deposited in the core to that in the full cone, for the sub-jets sj_1 and sj_2 , respectively
$p_T^{sj_2} / p_T^{LRJ}$ and $(p_T^{sj_1} + p_T^{sj_2}) / p_T^{LRJ}$	Ratio of the p_T of sj_2 to the di- τ seeding large-radius jet p_T and ratio of the scalar p_T sum of the two leading sub-jets to the di- τ seeding large-radius jet p_T , respectively
$\log(\sum p_T^{\text{iso-tracks}} / p_T^{LRJ})$	Logarithm of the ratio of the scalar p_T sum of the iso-tracks to the di- τ seeding large-radius jet p_T
$\Delta R_{\max}(\text{track}, sj_1)$ and $\Delta R_{\max}(\text{track}, sj_2)$	Largest separation of a track from its associated sub-jet axis, for the sub-jets sj_1 and sj_2 , respectively
$\sum [p_T^{\text{track}} \Delta R(\text{track}, sj_2)] / \sum p_T^{\text{track}}$	p_T -weighted ΔR of the tracks matched to sj_2 with respect to its axis
$\sum [p_T^{\text{iso-track}} \Delta R(\text{iso-track}, sj)] / \sum p_T^{\text{iso-track}}$	p_T -weighted sum of ΔR between iso-tracks and the nearest sub-jet axis
$\log(m_{\Delta R < 0.1}^{\text{tracks}, sj_1})$ and $\log(m_{\Delta R < 0.1}^{\text{tracks}, sj_2})$	Logarithms of the invariant mass of the tracks in the core of sj_1 and sj_2 , respectively
$\log(m_{\Delta R < 0.2}^{\text{tracks}, sj_1})$ and $\log(m_{\Delta R < 0.2}^{\text{tracks}, sj_2})$	Logarithms of the invariant mass of the tracks with $\Delta R < 0.2$ from the axis of sj_1 and sj_2 , respectively
$\log(d_{0, \text{lead-track}}^{sj_1})$ and $\log(d_{0, \text{lead-track}}^{sj_2})$	Logarithms of the closest distance in the transverse plane between the primary vertex and the leading track of sj_1 and sj_2 , respectively
$n_{\text{tracks}}^{sj_1}$ and $n_{\text{tracks}}^{\text{sub-jets}}$	Number of tracks matched to sj_1 and to all sub-jets, respectively

Comparison of Lumi for Single and Di-Higgs Searches

Analysis	Integrated luminosity (fb^{-1})	Ref.
$H \rightarrow \gamma\gamma$ (excluding $t\bar{t}H$, $H \rightarrow \gamma\gamma$)	79.8	[21,22]
$H \rightarrow ZZ^* \rightarrow 4\ell$ (including $t\bar{t}H$, $H \rightarrow ZZ^* \rightarrow 4\ell$)	79.8	[23,24]
$H \rightarrow WW^* \rightarrow e\nu\mu\nu$	36.1	[25]
$H \rightarrow \tau^+\tau^-$	36.1	[26]
VH , $H \rightarrow b\bar{b}$	79.8	[27,28]
$t\bar{t}H$, $H \rightarrow b\bar{b}$	36.1	[29]
$t\bar{t}H$, $H \rightarrow \text{multilepton}$	36.1	[30]
$HH \rightarrow bbbb$	27.5	[31]
$HH \rightarrow b\bar{b}\tau^+\tau^-$	36.1	[32]
$HH \rightarrow b\bar{b}\gamma\gamma$	36.1	[33]

Di-Tau Mass: Complications?

- ATLAS detects neutrinos only through **missing transverse momentum (MET)**
 - There is not a simple way to break down the total missing transverse momentum into the components from each neutrino.
- Various techniques have been used to take this difficulty into account:
 - **Missing Mass Calculator**
 - Collinear approximation
 - MOSIAC mass
 - Transverse/Partial masses



Missing Mass Calculator (MMC)

- In a nutshell: Uses a **likelihood** to require that the **neutrinos and other decay products** are consistent with the **mass and decay kinematics of a tau lepton**.
- Method: 6-8 unknowns
 - The x, y, and z components of missing energy associated with each tau lepton (6)
 - If including leptonic decays, the invariant mass of neutrinos from each leptonic decay (0-2, depending on decay mode)

- 4 Equations relate these unknowns:

x and y
components
of MET

$$E_{T_x} = p_{\text{mis}_1} \sin \theta_{\text{mis}_1} \cos \phi_{\text{mis}_1} + p_{\text{mis}_2} \sin \theta_{\text{mis}_2} \cos \phi_{\text{mis}_2}$$

$$E_{T_y} = p_{\text{mis}_1} \sin \theta_{\text{mis}_1} \sin \phi_{\text{mis}_1} + p_{\text{mis}_2} \sin \theta_{\text{mis}_2} \sin \phi_{\text{mis}_2}$$

tau mass

$$M_{\tau_1}^2 = m_{\text{mis}_1}^2 + m_{\text{vis}_1}^2 + 2\sqrt{p_{\text{vis}_1}^2 + m_{\text{vis}_1}^2} \sqrt{p_{\text{mis}_1}^2 + m_{\text{mis}_1}^2} - 2p_{\text{vis}_1} p_{\text{mis}_1} \cos \Delta\theta_{vm1}$$

Unknowns!

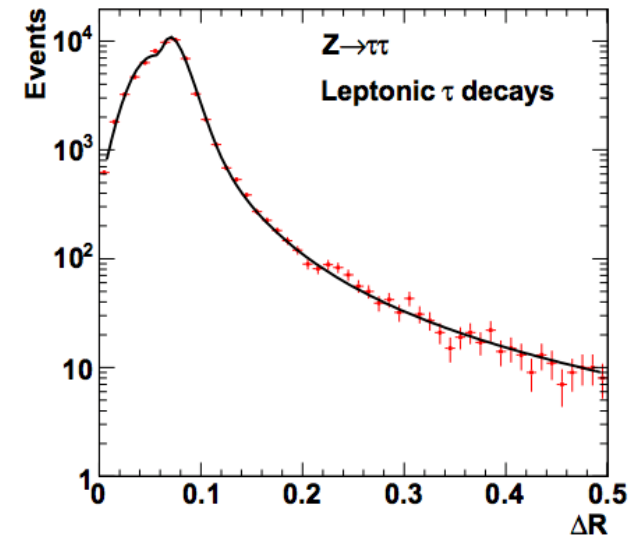
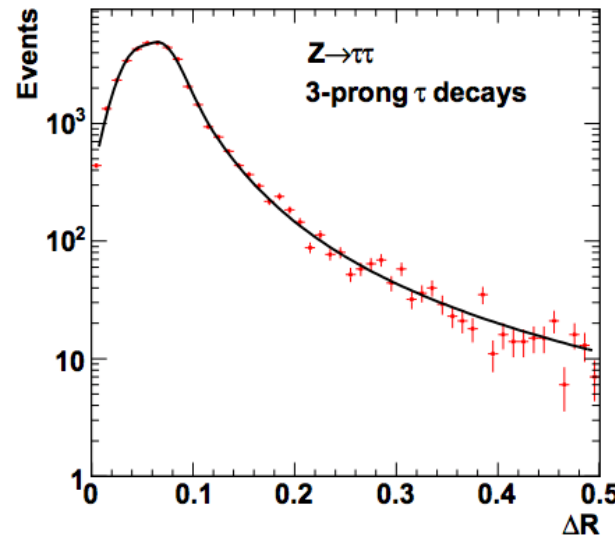
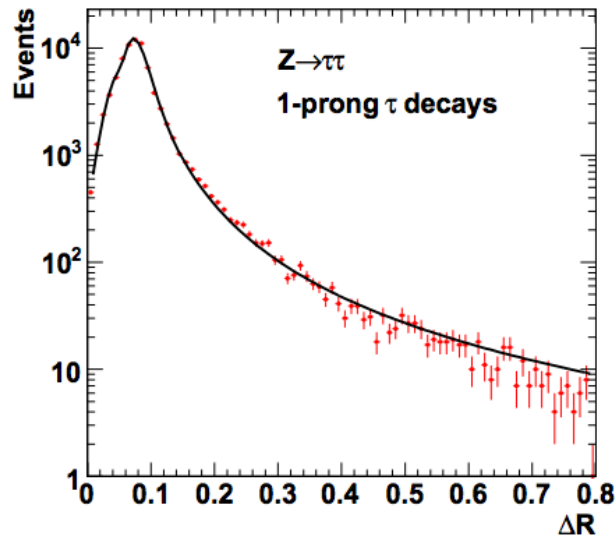
Momentum and
invariant mass of
visible tau decays

$$M_{\tau_2}^2 = m_{\text{mis}_2}^2 + m_{\text{vis}_2}^2 + 2\sqrt{p_{\text{vis}_2}^2 + m_{\text{vis}_2}^2} \sqrt{p_{\text{mis}_2}^2 + m_{\text{mis}_2}^2} - 2p_{\text{vis}_2} p_{\text{mis}_2} \cos \Delta\theta_{vm2}$$

Angle between
 p_{vis} and p_{mis}

Where do we go from here?

- With 6-8 unknowns and 4 equations, **system is under-constrained**.
- However, some solutions are more likely than others, given knowledge of the tau (e.g. ΔR between visible and invisible tau decay products).
- Additional knowledge of decay kinematics are incorporated as probability density functions in a global event likelihood, allowing a better estimator of $m_{\tau\tau}$.



Probability functions for three different tau decay types.

To A Likelihood!

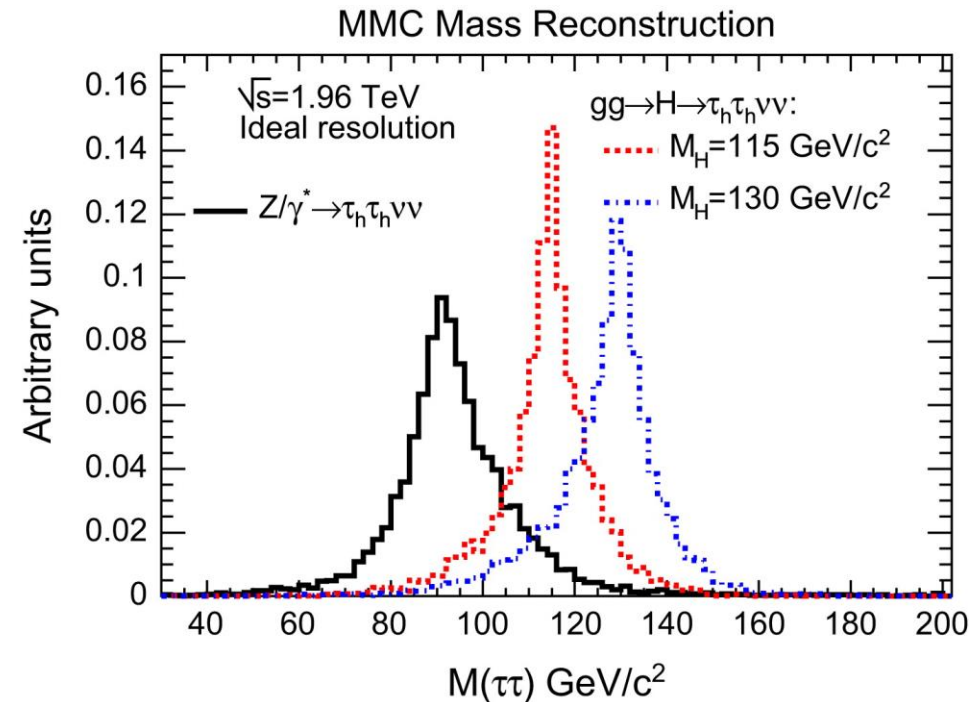
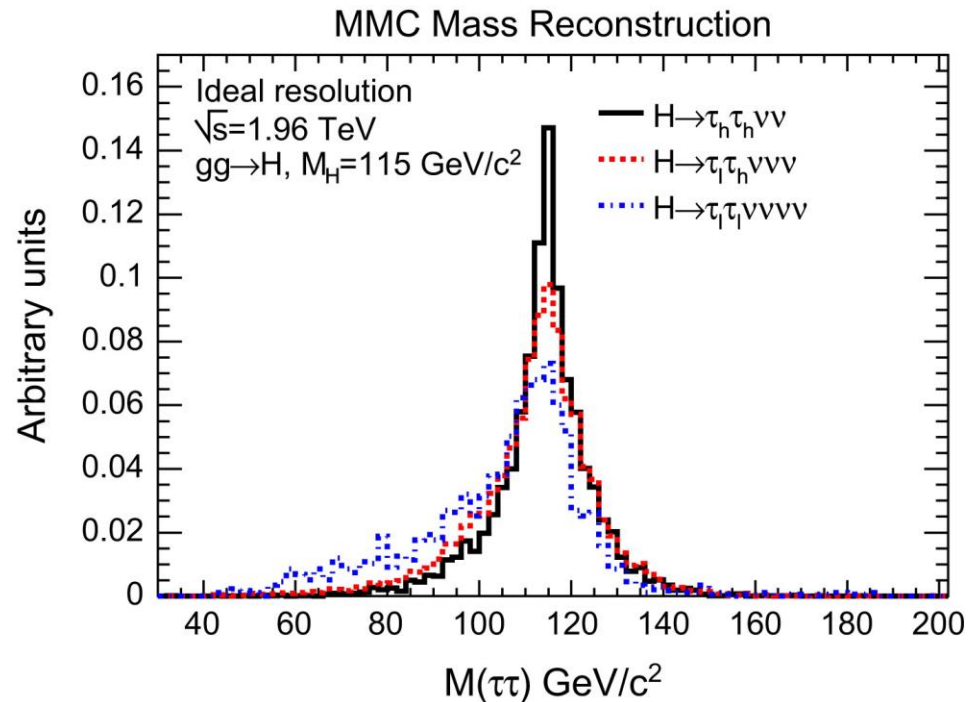
- Using ΔR as a constraint:
 - It is calculated using Pythia with TAUOLA, for each decay type and in τ p_T bins.
 - The distributions are parameterized using a linear combination of Gaussian and Landau functions.
 - These functions are defined as $\mathcal{P}(\Delta R, p)$, and are used to evaluate probabilities of particular decay topologies.
 - They are used to define an event probability (likelihood):

$$\mathcal{L} = -\log(\mathcal{P}(\Delta R_1, p_{\tau 1}) \times \mathcal{P}(\Delta R_2, p_{\tau 1}^2)),$$

- Example of use (2 hadronic decays):
 - Equations can be solved exactly for a given point $(\varphi_{\text{miss}1}, \varphi_{\text{miss}2})$
 - $M_{\tau\tau}$ is calculated for each point in a grid of $(\varphi_{\text{miss}1}, \varphi_{\text{miss}2})$, and weighted by a probability $\mathcal{P}(\Delta R_1, p_1) \times \mathcal{P}(\Delta R_2, p_2)$
 - The most probable value is chosen.
- For leptonic decays, grid is expanded in dimensionality as $(\varphi_{\text{miss}1}, \varphi_{\text{miss}2}, m_{\text{miss}1})$ or $(\varphi_{\text{miss}1}, \varphi_{\text{miss}2}, m_{\text{miss}1}, m_{\text{miss}2})$

Performance for a Perfect Detector

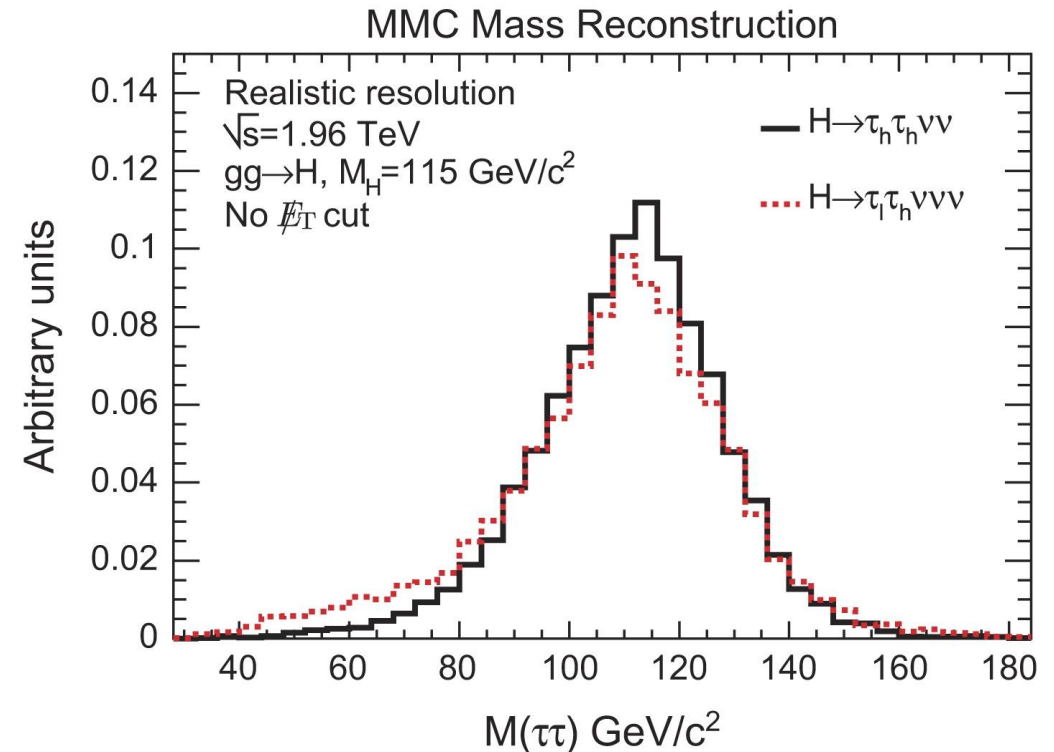
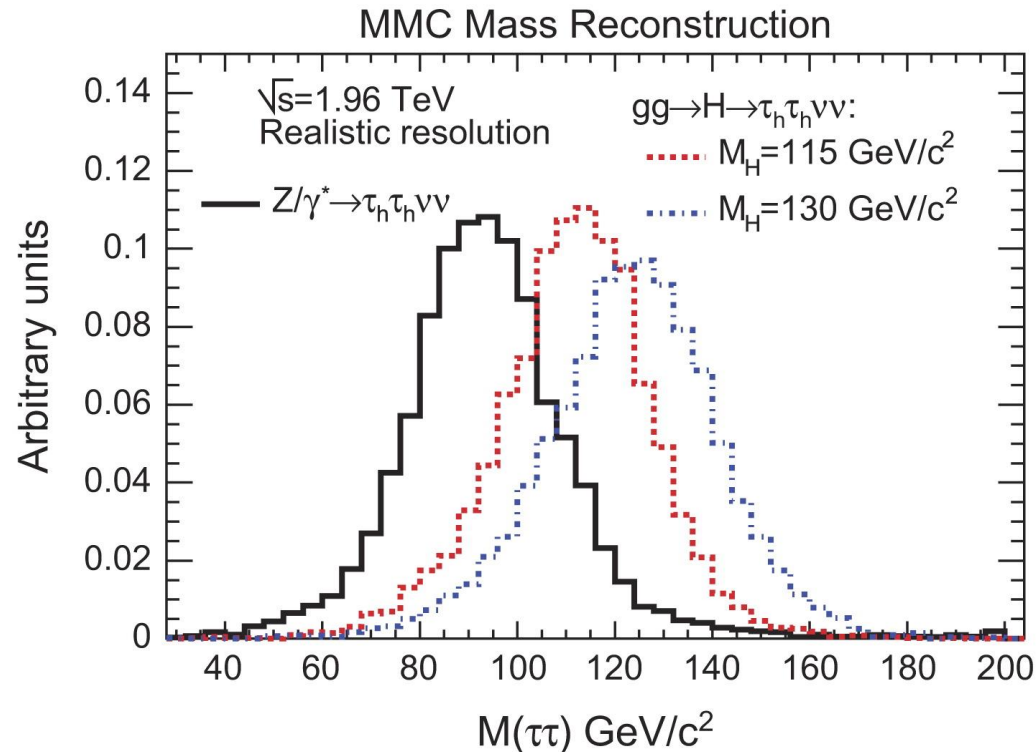
- Neglecting detector resolution, the method works very well!
- The best mass resolution is found for the 2-hadronic channel, which has the strongest constraints.



- Note: This method was established before the Higgs discovery, so plots will show a 115 GeV and 130 GeV Higgs boson.

Performance for an Actual Detector

- Incorporating detector resolution: 3 (10)% on momenta of e/μ (τ), and 5 GeV on MET
- Effects of MET resolution significantly reduce performance, so the likelihood is extended to allow for some MET mismeasurement.



Performance in $HH \rightarrow b\bar{b}\tau\tau$

